Reconstructing palaeoclimate and hydrological fluctuations in the Fezzan Basin (southern Libya) since 130 ka: a catchment-based approach

Reconstructing palaeoclimate and hydrological fluctuations in the Fezzan Basin (southern Libya) since 130 ka: A catchment-based approach

Nick A. Drake[a], Rachael E. Lem[b], Simon J. Armitage[c,d], Paul Breeze[a], Jan Francke[e,] Ahmed S. El-Hawat[f], Mustafa J. Salem[g], Mark W. Hounslow[h] and Kevin White[i].

[a]Department of Geography, Kings College, London, UK. nick.drake@kcl.ac.uk, paul.s.breeze@kcl.ac.uk
[b] School of Geography, Earth and Environmental Sciences, University of Plymouth, UK. rachael.lem@plymouth.ac.uk
[c]Department of Geography, Royal Holloway, University of London, UK.
[d]SFF Centre for Early Sapiens Behaviour (SapienCE), University of Bergen, Post Box 7805, 5020, Bergen, Norway. Simon.Armitage@rhul.ac.uk
[e] International Groundradar Consulting Inc. Toronto, Canada. jfrancke@groundradar.com
[f] Earth Sciences Department, University of Benghazi, P.O.Box 1308, Benghazi, Libya. elhawat@uob.edu.ly
[g]Earth Sciences Department, University of Tripoli, PO Box 13040, Tripoli, Libya. southlibya@gmail.com
[h]Lancaster Environment Centre, Lancaster University, Lancaster, UK. m.hounslow@lancaster.ac.uk
[i]Department of Geography and Environmental Science, The University of Reading, Whiteknights, Reading, UK. k.h.white@reading.ac.uk

Abstract

We propose a novel method to evaluate regional palaeoclimate that can be used to alleviate the problems caused by the discontinuous nature of palaeoenvironmental data found in deserts. The technique involves processing satellite imagery and DEM's to map past rivers, catchments and evaluate the areas and volumes of palaeolakes. This information is used to determine the new Lake Evaluation Index (LEI) that allows a qualitative estimate of the amount of sediment received by lakes and how long-lived those lakes are. Lakes with considerable longevity and large sediment stores are selected for study. Validation is performed using image interpretation of remote sensing data, UltraGPR surveys and fieldwork. These techniques are also used to identify and study spring deposits and fluvial landforms that provide valuable palaeoclimate information. The method is applied to the Fezzan Basin in southern Libya focusing on the Wadi ash Shati and Wadi el-Agial catchments. Results indicate that the palaeohydrology is accurately mapped except within dune fields. We analysed the sedimentology of the key deposits identified by this methodology, developing a chronology using optically stimulated luminescence (OSL) and radiocarbon dating. We find evidence for relatively humid conditions during MIS 5c/d and e, as well as during the early to middle Holocene. Larger lakes and more extensive river systems were present during MIS 5 than are found during the Holocene, suggestive of greater humidity. The Holocene humid period started at ~11 ka and continued until ~5 ka being interrupted by abrupt periods of aridity at ~8.2 ka and ~6 ka that coincide with North Atlantic cooling. After each of these arid events the climate was less humid than previously, suggesting that they were superimposed upon

an overall drying trend. The termination of the Holocene humid period in the Sahara has received much scrutiny in recent years, and sediments of Palaeolake Shati provide a continuous record of this. We do not find evidence to support the hypothesis of either sudden or gradual aridification of the Sahara at ~5 ka, instead we find that that aridity started to develop at ~6.5 ka, whereupon the lake levels oscillated until finally drying-up by 5.3 ka. Most of the other lakes in the Fezzan also dried up at ~ 5ka. We suggest that thousands of years of aridification prior to 5 ka shrunk these lakes so that additional aridity at this time led to their final desiccation. Because lakes are prodigious dust sources this mechanism potentially explains the rapid rise in dust flux to the Atlantic at 5 ka, with this final drying being the culmination of longer term aridity, albeit overprinted with considerable climate variability.

Keywords
Holocene, Pleistocene, Palaeohydrology, Paleoclimatology, lake evaluation index, Sahara, Middle East, Optical methods.

1 Introduction

Our understanding of past climate change in the Sahara has been predominantly informed by marine records (e.g. deMenocal et al., 2000; Tjallingii et al., 2008; Kuhlmann et al., 2004; Ehrmann et al., 2017) due to the continuous long-term records they provide. In contrast, terrestrial records tend to be discontinuous, having limited time duration due to deflation during periods of aridity. These problems become more acute for older records, for example there are around 610 dated Holocene Saharan palaeoenvironmental sites (Lezine et al., 2011; Street-Perrott et al., 1989) across an area of 10 million km^2, yet for Marine Isotope Stage (MIS) 5 there are only 44 (Drake et al., 2013). However, marine records of climate change derive their source particulates from large regions of the Sahara that are poorly defined. They are often referred to as representing 'the Sahara', suggesting that they provide information on the entire desert (e.g. deMenocal et al., 2000; Tjallingii et al., 2008), yet in reality which Saharan area that influences marine records is unknown. Furthermore, the nature of the sediment source is likely to have been affected by variations in climate and erosional deflation, producing a wide spatial range of aeolian and hydrological responses as a result of the diverse spatial geomorphological and environmental controls in the desert. Consequently, it is difficult to link marine records of climate change to environmental variations in specific regions of this vast Desert. The great advantage of terrestrial records is that they relate directly to the region from which they are derived, having been formed through directly acting aeolian, fluvial and lacustrine processes.

To alleviate the problem of incomplete preservation of terrestrial sediments we have developed a catchment-based method that relies upon studying the palaeohydrology of a region in an integrated manner; i.e. by considering a number of catchments, and by deriving palaeohydrological information from the full range of ancient waterlain sediments found within them (i.e. lacustrine, palustrine, deltaic, riverine and spring deposits). This approach provides a more complete record of climate change than studying any one landform or landform type in isolation. For example, lakes in different

geomorphological and hydrological settings have different sensitivities to changing water balance (Olaka et al., 2010; Street 1980) and thus may preserve different hydrological records. Furthermore, fluvial and spring deposits can also preserve important palaeoclimate information that can be used to augment that of palaeolake sediments (e.g. Matter et al., 2016; Pigati et al., 2014). Finally, the preservation of terrestrial sedimentary archives often varies according to hydrological location; for example, alluvial fans can prograde over palaeolake sediments, preventing subsequent deflation and resulting in preferential preservation of lake sediments where alluvial fans and palaeolakes are in close proximity. A catchment scale approach can help to identify these rare deposits of preserved lake sediments.

Assessment of the full set of waterlain sediments clearly has advantages in deserts, but, palaeolakes generally still provide the best palaeoclimate records (e.g. Kröpelin et al., 2008; Ritchie and Haynes 1987; Cremaschi and Zerboni 2009). Thus, the problem of applying our catchment-based approach becomes one of selecting catchments containing 'good' palaeolakes. This is important because some lakes preserve a considerable sediment records and exhibit good preservation, whereas others consist of condensed deposits that have been highly eroded, leaving only a few small mesas of sediment behind. Here we develop a Lake Evaluation Index (LEI) that permits those palaeolakes with the most promising palaeoclimate records to be determined from palaeohydrological mapping, allowing selection of their catchments for further study.

We apply this catchment-based method to the Fezzan Basin (Fig. 1). The Fezzan is well-suited to our analysis since it forms a giant closed basin (372,675 km^2) in the central Sahara, which hosted palaeolakes during past humid periods (e.g. Petit-Maire et al., 1980; Cremaschi and Di Lernia 1998; Armitage et al., 2007; Geyh and Thiedig 2008). These palaeolakes provide a wealth of palaeoclimate information, dating from the Miocene to the late Holocene, (e.g. Hounslow et al., 2017; Cremaschi and Zerboni 2009; Gaven et al., 1981; Petit-Maire 1982), making the Fezzan Basin unique in the central Sahara (Supplementary Information (SI) 1).

2 Methods

We map the palaeohydrology using the methods of Breeze et al., (2015), a technique using Geographical Information System (GIS) analyses of digital elevation models (DEMs) and satellite imagery to determine palaeolake areas and volumes, rivers and their catchments at a spatial resolution of 90 m (SI 2, Fig 1). We expand this methodology by using these data to calculate the LEI that provides a qualitative estimate of both the longevity of any lakes that develop when the climate becomes humid, and the amount of sediment that each palaeolake likely received. This allows prioritisation of palaeolakes for further study, with the prime targets being those with the greatest longevity and likely longest sediment record.

The LEI integrates numerous aspects of the palaeohydrology. Its rationale can be understood if we consider ideal desert palaeolake – one that fills early in a humid period and persists until the end of that period. Such palaeolakes tend to have small surface areas (a) in comparison to their volumes (v), since loss of water via evaporation from a lake is

principally controlled by its surface area, and the volume of the lake will determine the persistence of the lake when evaporation exceeds moisture input (e.g. Benson and Paillet 1989). Surface runoff is usually the most important source of water for lakes (e.g. Street-Perrott and Harrison 1985; Enzel 1992), particularly in semiarid basins where groundwater recharge and direct rainfall is often low (e.g. Yechieli and Wood 2002). Thus, persistent lakes will tend to have large catchment sizes (*s*), with more river discharge feeding into them. Lakes in larger catchments will also likely receive greater quantities of allogenic sediments (assuming load is related to discharge) and will thus tend to have higher sedimentation rates compared to lakes in smaller catchments. Furthermore, rivers that discharge from high mountains will provide more water and suspended sediment to lakes than those that are only fed by waters from lowlands, since highlands receive more rainfall due to orography (Mercuri 2008) and erosion is higher in steep mountainous terrains. Prior studies have demonstrated the importance of the 'water tower' effect of such central Saharan highlands (Lezine et al., 2011). This aspect of a palaeolakes catchment can be quantified by calculating its Hypsometric Index (h):

$$h = \frac{E_e - E_n}{E_x - E_n} \qquad \text{(equation 1)}$$

where E_e is the mean elevation, E_n the minimum elevation and E_x the maximum elevation.

Using these parameters, and their relationships described above, we propose the LEI whereby:

$$\text{LEI} = ((v/a)*s)*h \qquad \text{(equation 2)}$$

Larger values of LEI represent lakes that can be expected to experience high sedimentation rates, be the first to form during a humid phase, and be the last to dry up when it ends. Such lakes are likely to contain more sediment, and that sediment is likely to be submerged for longer, thus they are likely to contain the longest palaeoclimate records and be less affected by deflation in subsequent arid periods. Based upon LEI values calculated for mapped palaeolakes in the Fezzan Basin (SI 2 and Fig. 1b) we selected Palaeolakes Germa and Shati for further study. These palaeolakes are located in two of the largest catchments in the Fezzan Basin, those of the Wadi el-Agial and Wadi ash Shati (Fig 1a). They were chosen because they have high (el-Agial) and very high (Shati) LEI values, and thus should provide important palaeoclimate records as well as data to assess the utility of the LEI method.

The LEI only uses attributes of a palaeolake that can be readily estimated from a DEM and/or satellite imagery. It does not consider other regional controls, such as differences in precipitation and evaporation that are not controlled by elevation, or variations in groundwater inputs. Furthermore, though allogenic sedimentation rates can be expected to be higher in lakes with larger catchments and *h* values, biogenic sedimentation rates can be high in certain lakes, such as those that precipitate marls, and this factor is also not considered by the LEI. Given these potential limitations it is necessary to determine the advantages and limitations of the method. To do this we evaluated in detail its effectiveness for the Palaeolakes Shati and Germa, and for other lakes in the study area

when relevant information has been reported (see SI 1). This evaluation was performed by comparing each lakes LEI to their sedimentation rate and the timing of the termination of the lake at the end of the Holocene humid period. Lakes that have low LEI values are expected to have low sedimentation rates and to dry up earlier than those with higher values, hence the prediction is Paleolake Germa, that has lower LEI than Paleolake Shati, will dry up first and have a lower sedimentation rate.

The accuracy of the palaeohydrological mapping was evaluated by interpreting a suite of satellite imagery covering both these catchments (SI 2). When this interpretation was ambiguous, and where access was possible, these sites were investigated in the field and occasionally targeted for Ultra Ground Penetrating Radar (UltraGPR) survey in order to determine the sub-surface stratigraphy (SI 3). Field investigations also confirmed the location of key fluvial landforms, lake sediment outcrops and spring deposits. We then combined this information with previous palaeoclimate research in the region (SI 1) to identify sedimentary deposits likely to provide the most complete paleoenvironmental records. These sites were then visited, their stratigraphy documented, and samples collected for geochronological analysis using radiocarbon and Optically Stimulated Luminesence (OSL) dating (SI 4). In addition to this analysis of sedimentary outcrops, we recovered a 4 m sediment core from Holocene Palaeolake Shati (SI 5), to evaluate the unresolved question of if the termination of the Holocene humid period was abrupt or gradual (e.g. Kuper and Kröpelin 2006; de Menocal et al., 2000; Kuhlmann et al., 2004; McGee et al., 2013). Investigation of the core involved interpreting its stratigraphy, determining the gypsum crystal form, dating using OSL and analysis for phytoliths, particle size, chloride and sulphate content (SI 5).

3 Results

Palaeohydrological mapping in the Fezzan Basin identified 38,136 km of rivers that exceeded the 100 km^2 contributing area threshold level, and 816 palaeolakes (Fig. 1A) exhibiting a wide range of LEI values (Fig. 1B). Palaeolake Shati has the second highest LEI; the other lakes with high LEI are found near Murzuk. Palaeolake Germa yields the 14^{th} highest LEI. Those lakes with the lowest LEI values are generally found within sand seas. Palaeolakes Germa and Shati are discussed in turn below, along with the palaeohydrology of their catchments (the Wadi el-Agial and Wadi ash Shati catchments respectively).

3.1 Wadi el-Agial Catchment

Palaeohydrological mapping of the Wadi el-Agial (Fig. 1) indicates that the river system was 620 km long, rising at the southern end of the Messak Setaffet before flowing northwards along the base of the Messak escarpment. Numerous large tributaries feed the wadi from high in the Tasilli n' Ajjer and Acacus Mountains, the two largest having headwaters at elevations of 1800 m and 1200 m respectively. Because Saharan mountains generate major water sources during humid periods (see e.g. Mercuri 2008) these tributaries are likely to have been important components of the river system. When these tributaries emerge from the mountains they flow eastwards through the dunes of the Erg Uan Kasa to join the main channel of the Wadi el-Agial. This channel then flowed northwards until it was dammed by dunes of the Erg Uan Kasa, forming a palaeolake that

overflowed northwards into a channel flowing along the foot of the Messak Settafet escarpment, before being deflected eastwards by the impounding dunes of the Ubari Sand Sea. From here it continued along the base of the escarpment until it reached the town of Germa, terminating in a large palaeolake (Fig. 1). In a number of areas along the postulated river course, there is no visible evidence for this channel, either in the SRTM DEM, the satellite imagery (SI 2), or in the field. In these areas, the channel may have been obscured by subsequent geomorphic activity, but it is also possible that the mapped channel is erroneous in these places. To determine which of these possibilities is correct, we have used a number of techniques to determine whether the mapped channel exists in regions where no surface expression is present.

3.1.1 Validating the Palaeohydrological Mapping

Using satellite image interpretation, the channel can be mapped from its headwaters until it reaches a palaeolake dammed by dunes encroaching into the valley (Fig. 1). An outflow channel which cuts through the remaining dunes can be seen in the SRTM DEM emanating from the palaeolake. This channel then flows down the valley until it abuts against the dunes of the Ubari Sand Sea. The largest tributaries emanating from the Tasilli n' Ajjer and Acacus Mountains can clearly be seen cutting through the dunes of the Erg Uan Kasa (Fig. 2A), though the smaller ones are obscured by sand dunes. It is unclear whether they always terminated here, on the margins of the sand sea, whether they were blocked during Pleistocene or earlier arid periods, or whether they have been blocked with aeolian sand since the end of the Holocene humid period.

The course of the Wadi el-Agial river onwards from the Ubari Sand Sea is unclear. The first possibility is: If the dunes were absent in the past, or if the channel cut through them, it might have followed the slope of the land surface northwards, as proposed by Cremaschi (2001). Secondly: due to the presence of the dunes the channel was deflected eastwards, as the automated flow mapping suggests. Because this region is covered by small dunes, image interpretation shows no evidence of the channel to resolve which of these scenarios is most likely. However, 40 km further east the sand cover ceases, revealing an overfit palaeochannel 13 km long and 1.4 km wide, orientated east-west (Fig. 2B). Fieldwork shows this channel is bounded on each side by a ~1 m high terrace composed of sandstone bedrock and fluvial gravels. Thus, there is clear evidence for the westward deflection of the Wadi el-Agial river by the sand dunes of the Ubari Sand Sea at some time in the past, suggesting that the automated palaeochannel mapping in this area is correct.

The downstream end of the palaeochannel transforms from a large terrace-bounded feature into a braided channel system covering the entire valley floor between the Ubari Sand Sea and the alluvial fans draining the Messak Settafet escarpment (Fig. 2B). This change in channel style may have taken place because the palaeochannel was buried by later fluvial activity, or could simply result from a change in channel form.

3.1.2 UltraGPR Survey of Buried Palaeochannels

In order to determine if the channel is buried or not we conducted a UltraGPR survey over the gravel plain (SI 3). The majority of the UltraGPR transects across the valley

floor exhibit strong undulating reflections related to the fluvial gravels which extend from the surface to ~10 m depth. Beneath this there is an abrupt change to low amplitude, gently undulating, laminar reflections thought to represent the underlying Nubian Sandstone bedrock (Fig. 3A and B). The numerous small channels visible in the satellite images are not apparent in the radar data. This is partly due to their shallow depth; the top 1 m of the gravel plain is not imaged by the UltraGPR due to limitations of parallax between the widely-spaced radar receiver and transmitter, and the high amplitude first radar arrivals.

In some regions, the internal structure of this near-surface zone appears as layered laminar reflections that truncate the underlying fainter laminar reflections of the bedrock, suggesting in-filled palaeochannels (Fig. 3C). After applying amplitude equalizing and median filters to enhance the profiles, the stratigraphy becomes clearer (Fig. 3D). In this example, a strong coherent reflector is revealed through real amplitude processing, showing the presence of a palaeochannel. The normalized amplitude displays a second, deeper, channel beneath the strong reflector (Fig. 3E), incised into the sandstone to depths of at least 35 m. Interpretation of the cross-cutting relationships between the different reflectors suggests two sedimentary units, whereby a deep channel has been cut into a pre-existing palaeochannel sedimentary sequence (Fig. 3E). The strong reflectors at the base of this channel may represent layers of sand, which are stronger radar reflectors than gravel.

Across the gravel plain numerous similar palaeochannel features were detected by the GPR to depths of ~25 m. Because the gravel layer provides a distinct base to these profiles, its depth can be mapped confidently (Fig. 4A). Due to the sparse UltraGPR transect spacing, the data were interpolated in order to map changes in gravel depth over an area of 24x9 km (Fig. 4B). Since the radar profiles are spaced several kilometers apart, the deep zones are artificially stretched between adjacent radar profiles. Nevertheless, a large channel, over 200 m wide and 35 m deep, is evident in the UltraGPR. Other spatially restricted deep zones are also evident and are tentatively interpreted as areas of deep bedrock weathering. Thus, the UltraGPR profiles present compelling evidence for the existence of a large palaeochannel beneath the Wadi el-Agial. This channel is overlain by a thin layer of braided channel gravels, evident in the satellite imagery, which represents a later time interval with a differening style of fluvial activity.

The satellite imagery shows that the braided channel continues from the UltraGPR survey area until the town of Ubari (Fig. 1), after which it becomes obscured by human activity around the numerous oases between Ubari and Germa. The palaeohydrological mapping indicates that the Wadi el-Agial palaeochannel would have continued flowing eastwards from Ubari, before terminating in a palaeolake north of Germa (Fig. 1). Fieldwork in this region confirms the presence of palaeolake sediments.

3.1.3 Palaeoclimate Record of Wadi el-Agial Springs and Lakes

3.1.3.1 Spring-fed deposits

In the south-eastern part of the Wadi el-Agial there is evidence for large volumes of palaeodischarge from the Nubian Sandstone aquifer exposed along the base of the Messak Settafet. These springs produced an intermittent line of palustrine deposits along the base of the escarpment, which is exposed for 100 km from Germa to the region west of Ubari. (Fig. 5). These deposits superficially resemble palaeolake sediments, but are 75 m higher in the west than the east, and are not located in closed basins. The most extensive and thickest spring-fed palustrine sediments are located west of Ubari (Fig. 5). These deposits consist of a gypsum crust overlying fine grained grey marls inter-bedded with discontinuous layers of black organic-rich sediments. The latter two types of sediment contain fossil freshwater mollusks, *Melanoides tuberculata, Corbicula africana*, and less commonly *Bulinus truncatus*, indicating a perennially moist environment. AMS dating of the black organic-rich sediments provided a 2σ age range of 8.16 to 8.03 ka (Beta 210193, conventional radiocarbon age 7.29±0.04, calibrated age intercepts 8.11, 8.09 and 8.06 ka).

The spring-fed palustrine sediments become increasingly coarse grained towards the Messak Settafet, due to intermixing with material from alluvial fans, and eventually pinch out at the base of the escarpment. The stratigraphy of these deposits is complex, and the palustrine beds can only be followed a few hundred metres before they pinch out, or merge with sands and gravels deposited by channels on the piedmont. This can be explained by the lateral migration of river channels from the alluvial fans along the margin of a large spring fed marsh. The sediments were dated using both OSL (Table 1) and radiocarbon techniques. Three samples were collected for OSL dating from sands close to the palustrine layers, providing ages ranging between 11.3±1.0 and 9.2±0.6 ka (Armitage et al., 2007) (Fig. 6A) while a radiocarbon date of an organic rich layer is dated to 8.34-8.14 ka (Beta 210192, conventional radiocarbon age 7.40±0.05, calibrated age intercept 8.19 ka). While some discrepancies between OSL and radiocarbon ages are observed, overall these dates suggest significant spring discharge between ~11 and ~8 ka.

Similar sediments are found at the base of the escarpment just south of El Grafia (Fig. 6 B). The stratigraphy here consists of two cycles of fluvial gravels underlain by organic rich palustrine silts containing gypsum and the same suite of fossil mollusks found in section A. Thus, the stratigraphy suggests channel migration and the periodic evaporative concentration of spring waters. A single OSL age from palustrine sediments from this location (10.8±0.8 ka, Armitage et al., 2007) suggests that these materials are similar in age to the palustrine sediments west of Ubari. OSL dating of the second cycle of gravels shows that they are much older, dating to 52.8±6.2 ka. The underlying palustrine sands and organic silts are even older, dating to 119±10 ka (Fig. 6B). Thus, as with the site west of Ubari, there is evidence for spring activity in the early Holocene. However, at El Grafia a suite of much older sediments also indicate fluvial activity during MIS 3 and spring discharge during early MIS 5.

A different type of spring deposit is found further upslope within fissures at the base of the cliffs of the Messak at the junction between marl aquicludes and overlying sandstone aquifers (Fig. 7). These deposits are thought to have formed when the climate became more arid and the spring discharge was reduced to a trickle, leading to evaporative

concentration and gypsum precipitation (Brooks et al., 2003; Drake et al., 2004). ^{226}Ra dates of this gypsum define the onset of the late Holocene spring desiccation to around 5.5 ± 0.85 ka and the final desiccation at 3.1 ± 0.3 ka (Drake et al., 2004).

3.1.3.2 Palaeolakes

The Wadi el-Agial palaeochannel terminates in Germa palaeolake, which is fed from both fluvial and spring sources. We excavated trenches from the margin towards the center of the lake, which revealed red lacustrine silts with intergrowths of gypsum near the surface, overlying aeolian sands (Brooks et al., 2003; Drake et al., 2006; Fig. 7). This stratigraphy indicates that after a period of aridity indicated by the presence of the sands, the lake levels rose, depositing red lacustrine silts and clays, after which lake levels dropped, causing evaporative concentration and growth of lenticular gypsum crystals in the near surface sediments. OSL dating of basal silts suggests that there was a lake low stand at 5.9±1 ka, while U/Th dating of gypsum indicates that the onset of dry conditions occurred from 4.0±0.2 ka (Fig. 7) (Brooks et al., 2003; Drake et al., 2006). ^{226}Ra dating of the gypsum generally supports these U/Th results, with an age estimate of 3.7±0.2 ka for this final desiccation event (Drake et al., 2004). The termination of the lacustrine cycle in the Wadi el-Agial at ~4.0-3.7 ka is consistent with the evidence from the spring deposits described above.

3.2 Wadi ash Shati Catchment

Mapping of palaeohydrological features shows that the Wadi ash Shati catchment is roughly circular, with Palaeolake Shati at its centre being fed by numerous rivers. The palaeochannel system feeding the lake can clearly be seen by remote sensing and field validation, with the exception of the Ubari Sand Sea to the south. The apparent lack of influent palaeodrainage from the Ubari Sand Sea may be due to sand movement and deflation since this region last became arid.

Wadi ash Shati received groundwater discharging from the Cambrian-Ordovician and Devonian sandstones. However, the lack of significant spring fed palustrine deposits surrounding the lake suggests that past groundwater discharge was much less significant than in Wadi el-Agial. Consequently, the palaeoclimate record here consists predominantly of lacustrine sediments assigned to the Shati Formation (Hounslow et al. 2017). An extensive area of Holocene lake sediment is preserved at the base of the Wadi ash Shati depression, which have been clearly defined by the palaeohydrological mapping. Remnants of Late Pleistocene deltas and lake sediments are also preserved around the margins of the lake at higher elevations (see below).

3.2.1 Pleistocene Palaeolake Sediments: *Coquinas*

Numerous small coquina deposits (1 to 200 m in outcrop length) belonging to the Aqar Member of the Shati Fm (Hounslow et al., 2017) occur in bioaccumulations on the margins of Palaeolake Shati. These predominantly consist of *Cerastoderma glaucum*, a brackish water bivalve that can tolerate a wide range of salinities. It is found associated with brackish-water Ostracoda *Cyprideis sp*. and several saline water foraminifera, thus indicating the presence of a brackish lake with fluctuating salinity (Gaven et al., 1981). These deposits have been OSL dated to 98±7, 107±8 and 108±9 ka (Armitage et al.,

2007), suggesting they were deposited in MIS 5c and d. The largest coquina deposits retain a large-scale cross-bedded shell bar sedimentary structure that indicates deposition in a high-energy lacustrine shoreline environment. Their thickness was controlled by the topography of the Palaeozoic substrate upon which they largely rest. The largest outcrop retains a bar-shaped morphology, up to 200 m long, 12 m high, and oriented in an east-west direction, parallel to the palaeoshoreline. The stratigraphy of this deposit, and that of a smaller outcrop nearby, were described and palaeocurrent directions measured for subsequent analysis (Fig. 8).

Stratigraphically, the main deposit (Aqar 2 in Fig. 8) consists of two stacked coarsening-up and shallowing-up sequences that document lake level oscillations. The basal unit forms a coarsening-up tripartite cycle consisting firstly of grayish-green clays and sandy siltstone, mixed with floating shell fragments, interpreted as profundal lacustrine sediments deposited below storm wave base. The second cycle forms a series of thin, thinning-up tempestite layers consisting of shell fragments grading into a sandy siltstone that suggest deposition during high-energy events at or above storm wave base. The final cycle is a sandy shell rich mudstone mixed with pebbles reworked from the Devonian substrate. This cycle is thought to have been formed when the lake level was rising, as illustrated in the depositional model shown in Supplementary Fig. 1A. It is overlain by a sequence consisting of a thick *Cerastoderma glaucum* shell bank that is mainly composed of articulated bivalve shells passing laterally into sets of prograding coquinoid clinoforms and back bank spill-over lobes. This sequence is interpreted as having accumulated during the lake high-stand (Supplementary Fig. 1B and C). The final sequence consists of prograding cross-beds interpreted as a shallowing up and coarsening up shoreface deposit. The basal erosional boundary is sharp, and is followed by thin bioclastic tempestite layers overlain by a series of low angle inclined cross-bedded sets. The succession is capped by a crossbedded shell debris bed intermixed with reworked sandstone and siltstone pebbles. These features suggest a high-energy channelised foreshore facies deposited during a lacustrine low-stand soon after the lake contracted (Supplementary Fig. 1D).

The nearby coquina deposit (Fig. 8, Aqar 1) is a few metres higher, thus nearer the lake shoreline, providing a proximal shallow water section. Aqar 1 is much smaller than Aqar 2 because of the reduced accommodation space, but the same three sequences can be recognized within it. The altitude of this deposit, and that of the deeper water deposit at Aqar 2, varies between 342 and 333 m, suggesting that the height of the lake shoreline was around 340 m. Extrapolating this lake altitude with the DEM provides a lake area estimate of 1663 km^2 (Fig. 9A).

Statistical analysis of the cross-bedding palaeocurrent indicators in the top sequence at Aqar 2 yields a polymodal rose diagram (Fig. 8) with an E-W bimodal trend and north unidirectional group. However, grouping of data according to locality, and the type of sedimentary structures produced by bedforms, provides more insight. The shallow water deposits of the Aqar-1 section are dominated by a northward (shoreward) flow direction that is spread over 130^o and reflects the irregularity in the shoreline rocky substrate (Fig. 8). These shoreward migrating bedforms are associated with a minor low angle westward

transport direction. In contrast the giant bar-shaped bioaccumulation, exposed in the lower parts of the Aqar-2 section, was deposited in deeper water that offered more accommodation space. Its sedimentary structures yield a trimodal rose diagram (Fig. 8). The ESE trending mode represents the high angle (025^{o}) prograding clinoforms of the lee side of the bar. A western low angle cross-bedded set (mode 005^{o}-010^{o}) represents its stoss side. The third mode is a minor northerly shoreward transport element. The easterly lateral accretion suggests persistent transport of the large coquinoid bodies by a longshore current indicative of waves generated by a predominant westerly wind. The palaeocurrent readings appear to show that the breaker wave line was striking in a direction of 032^{o} and moving in a due east direction (099^{o}). This westward flow direction is likely to have been caused by Atlantic westerly lows and suggests that these weather systems reached a latitude 4^{o} further south than they do today. These are winter rain bearing weather systems, and thus it is possible that part of the humidity in the Wadi ash Shati catchment during this MIS 5c lake phase can be attributed to moisture supplied by such systems.

3.2.2 Pleistocene Palaeolake Sediments: *Deltas*

The 340 m altitude shoreline of Palaeolake Shati extracted from the DEM features a notable protrusion near its south-eastern end (Fig. 9A). In this region, the DEM reveals two river valleys emerging from under the Ubari Sand Sea, each with delta shaped features at their mouths (Fig. 9B). The western delta has a birds-foot form and is at the same altitude (340 m) as the MIS 5c coquinas, indicating it was active during the same interval. The eastern channel has a more irregular delta system, consisting of two broad delta lobes at an altitude of ~335m (Fig. 9B), indicating that this delta formed at a slightly lower lake level. Both deltas comprise sediments consisting of sands and gravels containing *Cerastoderma glaucum*, and more minor *Corbicula africana*, *Bulinus trancatus* and *Limnaea natalensis* components. Petit-Maire et al., (1980) reported *in-situ* Levallois flakes in the central lobe of the eastern delta, and we targeted this region to study both the delta sediments and lithic artefacts. Transects on the eastern and western sides of the delta lobe revealed extensive Middle Palaeolithic-style artefacts on the surface (Lahr et al., 2008). Two 1.5 metre deep pits were excavated, yielding similar stratigraphy, consisting of a superficial disturbed surface above a thick layer of moderately calcified sand containing numerous *Cerastoderma glaucum* fragments. This sand is underlain by a layer of larger pebbles and cobbles, below which is coarser sand. This stratigraphy is similar to that reported by Petit-Maire et al., (1980). One artefact (a flake) was recovered from the pebble layer, demonstrating the presence of humans prior to deposition of the shell rich level. In the eastern pit the shell layer yielded an OSL age of 126±8 ka (Table 1 sample FZ75), while the same layer in the western pit yielded an age of 133±10 ka (Table 1 FZ77). These ages suggest that the shell layer was deposited around the MIS6/5 transition. Thus, the eastern delta appears to be both older and lower than the western delta. GIS analysis of the DEM suggests that a lake with a shoreline at an altitude of 335 m would have an area of 1342 km^2, 321 km^2 smaller than the lake associated with the coquinas and western high-stand delta.

Gaven et al., (1981) also reported sand and gravel rich sediments at the eastern end of Wadi ash Shati, but did not recognize them as deltaic deposits. The mollusk assemblage and its isotopic composition, show that they grew in less brackish water than the coquina

deposits detailed above, supporting the deltaic origin of these deposits. Furthermore, quartz pebbles derived from Nubian Sandstone of the Messak Settafet, suggest that the river that fed the delta came from the south, consistent with the geomorphology of the deltas and the alignment of the river channels that feed them. The largest river channel in this region is the Wadi el-Agial, and our interpretation of both the palaeohydrology and topography suggests that this river was connected to Palaeolake Shati. During MIS 5c and e there must have been enough water in the wadi to fill Palaeolake Germa, which in turn overflowed eastwards along the base of the escarpment, filling the two other mapped palaeolakes (Fig. 1). At the town of Sabah the channel would have turned northwards, continuing through the dunes of the Ubari Sand Sea for a further 95 km before terminating in the Wadi ash Shati deltas. Thus it would appear that Wadi el-Agial was one of the main sources of freshwater for Palaeolake Shati during MIS 5.

3.2.3 Pleistocene Palaeolake Sediments: Diatomites

Lake Sediments are also found preserved under alluvial fan gravels on the northern margin of Palaeolake Shati, at an altitude of 296 m (Fig. 6 C). The base of the section consists of a layer of large (~5 cm) lenticular gypsum crystals overlying a Carboniferous shale. Above this is a diatomite, a monospecific assemblage of *Actinocyclus normanii f. subsalsu*s (Gasse Pers. Comm.). The diatomaceous sediments are gypsiferous at their base, but grade into a thicker bed of pure laminated diatomite that becomes more gypsiferous again towards the top, where it is capped by a layer of lenticular gypsum crystals. The gypsum is overlain by a layer of silt, and then clay, both of which contain nodules of lenticular gypsum. This unit is overlain by gravel and cobbles of the alluvial fan, cemented by halite in places.

Lenticular gypsum crystals are found throughout the section; this crystal form indicates that they grew in saturated groundwaters (Cody and Cody 1988), and are thus post-depositional. *Actinocyclus normanii f. subsalsu*s, lives in marine and brackish waters, indicating high salinity. It is a heavily silicified deep water species, and needs turbulent mixing of the water to keep it in the photic zone, therefore indicating that it was deposited in a deep well-mixed saline lake. The overlying sediments are interpreted as being deposited during a falling stage of the lake level, as its contraction brought the deposit closer to the lake margin where it received fine grained sediments from the nearby alluvial fans. Over time the adjacent fan prograded over the desiccated lake surface, depositing gravels that were subsequently cemented with halite derived from groundwater in the underlying lake sediments, the same waters that precipitated the gypsum found throughout the section.

We attempted OSL dating of three different lacustrine units. The diatomite contained no dateable minerals. The overlying silt yielded an OSL age of 123±9ka (Table 1, sample FZ79), whilst the OSL signal in the overlying clay is saturated (Table 1, sample FZ78). Given the large uncertainty associated with FZ79, it could belong to either of the two lake phases outlined above. However, it is closer in age to the low-stand delta of Palaeolake Shati, thus the most parsimonious interpretation is that these sediments were deposited towards the end of the low-stand delta lake phase.

3.2.4 Holocene Palaeolake Sediments

At the base of the Wadi ash Shati is a gypsum-covered Holocene playa with a surface area of 210 km^2. This is considerably smaller than the lakes that existed during MIS 5. Our palaeohydrological modelling suggests that the Wadi el-Agial river did not reach Palaeolake Shati during the Holocene, which is confirmed by the lack of evidence for a Holocene delta on the margins of Palaeolake Shati. Thus, the smaller Holocene lake most likely indicates that the environment was not humid enough to produce the extensive hydrological networks that existed at times during MIS5.

To gain an insight into Holocene climate change we obtained a 4 m core from near the center of the Wadi ash Shati basin (SI 5). The base of the core is dominated by clays, while the top 2 m consists of inter-bedded layers of clays and gypsum (Fig. 10). Iron rich horizons were also observed at depths of between 356 cm and 325 cm and from 342.5 cm to 300 cm. Three types of gypsum were identified in the core, and were classified according to Cody and Cody (1988) as lenticular, prismatic, and desert rose. Prismatic gypsum crystals are deposited from evaporating lake waters, and thus formed during lake desiccation events, whilst lenticular and desert rose gypsum precipitate from groundwater and signify past water table fluctuations. Analysis of gypsum crystal form showed that the gypsum layers between 60 -75 cm and 300-350 cm depth are lenticular groundwater precipitated gypsum, and thus a post-depositional addition to the sediments, whilst all the gypsum horizons consisting of prismatic gypsum must have formed during evaporative concentration of lake waters and therefore represent lake-level fluctuations contemporaneous with sedimentation. Chloride (Fig. 11) and sulphate (Fig. 11) are found throughout the core, but are generally found at higher concentrations in the gypsum layers. The continuous presence of these ions indicates that the entire core has been affected to some extent by groundwater, but concentrations are highest when prismatic gypsum was precipitating as the lake waters became saline. The top of the core is capped by a bed of pure prismatic gypsum that contained no phytoliths or clastic sediments.

OSL dating of the Wadi ash Shati core yielded a suite of ages spanning 7.4±0.6 to 5.3±0.4 ka, with occasional stratigraphic inversions (Fig. 10). It is possible that these age inversions relate to post-depositional incorporation of gypsum, which contains uranium in disequilibrium, and may result in erroneous environmental dose rate estimates. However, there is a broad consistency to the OSL ages, and a Bayesian age-depth model produced using OxCal v4.2 (Bronk Ramsey 2009) did not identify any outliers (Supplementary Fig. 2). Based on this age model, the base of the core was deposited at about 7.4±0.4 ka whilst sedimentation ceased at 5.3±0.3 ka (Fig. 11). We interpret the clays to have been deposited in a perennial lake environment which existed from before 7.4±0.4 ka to 6.6±0.2 ka, with the sandy layers representing coarser material brought in by exceptional flood events (Fig. 11). The relatively thick and pure prismatic gypsum bed overlying the clays, that was deposited between 6.6±0.2 ka and 6.±0.2 ka, indicates that the lake became saline during this period, as the climate became more arid. This was followed by further deposition of clay, suggesting a return to less saline conditions, then deposition of three thin gypsum rich beds, separated by clays, suggesting oscillations in lake water salinity between 6.3±0.2 ka and 5.8±0.2 ka. The resumption of clay deposition that followed represents the final freshwater lacustrine phase before deposition of a thick

gypsum bed from 5.6±0.3 to 5.3±0.3 ka, whereupon the lake dried up. These salinity fluctuations suggest that aridification started at 6.6±0.2 ka and consisted of a series of arid/humid oscillations before the onset of permanent aridity at 5.3±0.3 ka.

Phytoliths are present throughout the core (Fig. 11). Both tree and grass phytoliths are found at its base, with the latter being more abundant, suggesting a sparsely wooded savannah environment. There are fluctuations in the proportion of tree phytoliths between 7.4±0.4 and 6.7±0.2 ka, after which they are only found in low numbers until they cease at 6.5±2 ka. Grass phytoliths are found throughout the core. From this we infer that soon after the first prismatic gypsum bed is deposited at 6.6±0.2 ka, trees disappear, and grass then dominates. Both of these proxies suggest instigation of a dry climate at this time.

4 Discussion

4.1 Validation of Paleohydrological Mapping

Validation of the palaeohydrological mapping using remote sensing data demonstrates that it is effective for understanding past desert hydrological systems. However, verification of the hydrological maps is difficult in dune fields, where recent aeolian activity can obscure past fluvial activity. Spurious lakes may also be identified in 'holes' in the SRTM DEM. Furthermore, the HydroSHEDS data that we used to map the rivers (SI 2) tends to produce long interconnected channels in interdune depressions by cutting through small dunes, which often produces an unrealistically high drainage density. In some areas there is evidence that these channels existed (e.g. Fig 2a), and in others there is not, so channels mapped in dune fields need to be treated with caution. However, outside dune fields, this tendency of HydroSHEDS to cut through small dunes is beneficial where recent small dunes cut across older channels. Despite these issues, the Wadi el-Agial channel crosses four dune regions, and yet our verification studies demonstrate that it was accurately mapped. Consequently, we are confident that the main hydrological features of the study area have been correctly identified. Interestingly, the Wadi el-Agial channel shows different behaviors when it interacts with different dune fields. In the Erg Uan Kasa the river cuts through the sand dunes, whereas in the Ubari Sand Sea the dunes deflect the channel to the east. This might be due to a steeper regional gradient in the Erg Uan Kasa.

4.2 Palaeoclimate Record

4.2.1 Late Pleistocene

The studied palaeolake deposits provide a rich record of past climate change, with the existence of Palaeolake Shati during MIS 5 being recognized previously (Gaven et al., 1981; Petit-Maire 1982; Armitage et al., 2007). However, we demonstrate that there were two lake phases, a large lake in MIS 5c and d and a slightly smaller one during the older MIS 5e. This older lacustrine phase coincides with evidence for spring discharge in Wadi el-Agial, and it is probable that some of the water that fed Palaeolake Shati came from the Tasilli n' Ajjer and Acacus mountains, via the Wadi el-Agial, presumably originating from enhanced monsoonal rainfall (Cremaschi et al., 2010). However, the palaeowind directions obtained from the coquina deposits suggest that Atlantic westerly lows may have provided water to the northern part of the Fezzan catchments. If this is the case, Atlantic westerlies extended 4^{o} further south than they do today, and the catchment may

then have received year-round rainfall, both from the summer monsoon and winter westerlies, perhaps explaining the presence of a large lake at this time.

The Late Pleistocene lakes in Wadi ash Shati are much larger than those found during the Holocene, probably due to higher humidity, driven by stronger precessional maxima (Shanahan et al., 2015), although changes in palaeohydrology probably also played a role. Deltas on the margins of Palaeolake Shati demonstrate fluvial input from Wadi el-Agial during parts of MIS 5, connecting the two catchments studied here. The large buried palaeochannel found under the gravel plane west of Ubari is currently undated, but given that the two relict deltas on the margins of Palaeolake Shati formed during MIS 5c/d and e, and the fact that the channel appears to exhibit two phases of deposition, we tentatively attribute the deeper channel to MIS 5e, and the shallower one to MIS 5c/d. The fluvial system that subsequently buried these channels is probably Holocene in age, and would have provided the silts and clays deposited in Palaeolake Germa. Evidence of increased humidity in MIS 5c/d and e is consistent with the other MIS 5 terrestrial records in the Sahara, which also indicate the presence of palaeolakes during these periods (Drake et al., 2013; Nicoll 2017).

The Wadi el-Agial forms part of a hypothesized riverine/lacustrine corridor for dispersal of humans and other animals across the Sahara and 'out of Africa' (Drake et al., 2008; Drake et al., 2011). The presence of Middle Palaeolithic-style artefacts at the low stand delta in Wadi ash Shati (Lahr et al., 2008; Petit-Maire 1980) demonstrates that humans were living on the margins of the lake during MIS 5e, showing that palaeolake shorelines were suitable environments for human occupation.

There is a paucity of evidence for humidity in the study area between MIS 5c and the Holocene, apart from a single date (~53 ka) from alluvial fans emanating from the Messak Settafet escarpment. This deposit might represent enhanced rainfall, but could equally be caused by ephemeral flows from occasional storms, such as those that periodically occur today. Though some Atlantic marine records indicate Saharan humidity at this time (e.g. Castaneda et al., 2009 at 50-45 ka), there is a dearth of continental records during this period. The only North African records indicating humidity at this time are from the eastern Sahara, the palaeolake at Bir Tirfawi (Nicoll 2017) and spring tufas at Kharga Oasis (Sultan et al., 1997) and Wadi Abu Had-Dib (Hamdan 2000) in Egypt. There is no unambiguous evidence for humidity from the central and western Sahara.

4.2.2 The Holocene Humid Period

During the early Holocene there is a rich record of climate change from both springs and lakes. Considerable spring discharge in the northern Wadi el-Agial catchment occurred between ~11 and ~8 ka, forming extensive palustrine deposits. Spring tufa formation in the nearby Acacus Mountains appears to have started by 9.6 ka but finish at around the same time (~8.1 ka; Cremaschi et al., 2010), with cessation of tufa formation attributed to the well-known and widespread 8.2 ka aridity event (Alley et al., 1997). In the Wadi el-Agial, this arid event appears to have marked the end of formation of palustrine deposits caused by a reduction in spring discharge. Evidence for the 8.2 ka arid event is also found

in the interdune basins of the Murzuk Sand Sea where lake levels fell (Cremaschi and Zerboni 2011). Increased aridity at ~8.2 ka is not restricted to the Fezzan basin, but is widespread in the Sahara (e.g. Gasse 2000; Zielhofer et al., 2017), further afield in North Africa (e.g. Gasse 1977; Shanahan et al., 2006; Marshall et al., 2011) and globally (e.g. Alley et al., 1997; Mayewski et al., 2004).

The lacustrine sediment record of Palaeolake Shati starts at ~7.4 ka, when there is evidence for a permanent lake set in a sparsely wooded grassland environment. However, the lake becomes saline at ~6.6 ka and trees cease to be a prominent part of the landscape at about 6.5 ka, never to return. The lake becomes less saline at ~6.3 ka, after which a series of arid/humid oscillations occur, before the lake finally dried up at about 5.3 ka. At Palaeolake Germa the record starts at 6 ka, when there is evidence for a lake low stand followed by a larger lake until desiccation at 3.7 ka (Drake et al., 2004). The dryer phase at 6 ka coincides with an arid event in Palaeolake Shati at ~6.1 ka and a final drying of lakes in the Murzuk Sand Sea (Cremaschi 1998; Cremaschi and Di Lernia 1998).

Similarly, in the Tassili N'Ajjer Mountains the *Cupressus dupreziana* dendrochronology record shows an arid phase centered at ~6 ka (Cremaschi et al., 2006), and in addition the archaeology of the Acacus suggests a hiatus at settlement sites at this time (Grandi et al., 1998). Despite the strong evidence for an arid period in the Fezzan at ~6 ka, evidence for aridity at this time in the wider Saharan record is sparse, being limited to a recently reported record from Morocco (Zielhofer et al., 2017). Certainly the ~6 ka arid phase is not as well documented as that at ~8.2 ka. However, a number of sub-Saharan records do indicate aridity at ~6 ka, notably at Lake Mblalang in northern Cameroon at 6 ka (Nguetsop et al., 2011), the Gulf of Guinea at 6.2 ka (Weldeab et al., 2005), in East Africa at Lake Victoria at 6.3 ka (Mayewski et al., 2004) and at Mt Kilimanjaro at 6.1 ka (Thompson et al., 2002). Surrounding regions also yield evidence for aridity at this time, such as in the Dead Sea at 6.1 ka (Migowski et al., 2006), the Mediterranean Sea at 6.2 ka (Rohling et al., 2002), the Arabian Sea centered on 6.0 and 6.1 (Gupta et al., 2003) and southern Oman at 6.0 ka (Fleitmann et al., 2003). In the Fezzan the long-term effects of this event appears to be spatially variable. Palaeolake Germa recovered while lakes in the Murzuk Sand Sea did not, though lakes continue to exist in the Erg Uan Kasa. Palaeolake Shati only partly recovered, changing from a permanent freshwater lake to one that experienced large salinity fluctuations. These differences are best explained by differences in groundwater inputs. The fact that after both the 6 and 8.2 ka events, some areas record a permanent shift to lower moisture availability suggests that these arid events occur within a more general drying trend. This can be explained by the southward migration of the monsoon in response to declining summer insolation. Both the ~6 and 8.2 ka events coincide with North Atlantic Ocean cooling (Bond et al., 1997) suggesting that changes in Atlantic Ocean temperature also had a widespread effect on monsoon strength, as also recognized by others (e.g. Zielhofer et al., 2017; Gasse 2000).

4.2.3 The Onset of Aridity

The final desiccation of Palaeolake Shati at ~5.3 ka coincides with the drying of the last lakes in the Erg Uan Kasa at ~5 ka (Cremaschi and Di Lernia1999; Cremaschi 2001) and accords with a considerable body of research documenting aridification of the wider

Sahara at this time (Zielhofer et al., 2017; Armitage et al., 2015; deMenocal et al., 2000; Kuhlmann et al., 2004; McGee et al., 2013). However, the rate of desertification is a controversial issue. Some find evidence for rapid drying attributed to nonlinear response of the monsoon to insolation forcing (e.g. deMenocal et al., 2000; Armitage et al., 2015). Others argue for gradual change from savannah to desert over a few thousand years (e.g. Kröpelin et al., 2008; Ritchie and Haynes 1987). The Palaeolake Shati sediment record allows evaluation of this issue in the central Sahara, but supports neither theory, showing a more complex trend in which the first evidence of a drying environment occurs at ~6.5 ka when the lake becomes saline and trees disappear from the landscape. After this the lake experiences a series of salinity oscillations until the final onset of desert conditions at about 5.3 ka.

Castañeda et al., (2016) show that the controversy over the rate at which the modern Sahara Desert was established is, in part, due to differences in the sensitivities of the proxies employed to measure it. However, when using lacustrine records, these discrepancies can also be caused by the different hydrological characteristics of the lakes involved. While the final drying of lakes in Wadi Shati at about 5.3 ka coincides with the desiccation of the lakes in the Erg Uan Kasa (Cremaschi and Di Lernia1999; Cremaschi 2001), it occurs about 1.5 ka before Palaeolake Germa dries. This lag can be attributed to groundwater buffering, since Palaeolake Germa disappears soon after spring discharge in the vicinity ceases (Drake et al., 2004). A handful of other palaeolakes in the Fezzan appear to have survived until this time. For example, Cremaschi (2001) dates the final desiccation of lakes in the Erg Tanezzuft to 3.55±0.08 ka and a small number of groundwater fed lakes survive in the Ubari Sand Sea today. Consequently, differences in groundwater buffering and catchment characteristics are very likely to produce differences in lake records, as has been recognized elsewhere (Olaka et al., 2010, Street 1980). Given these issues it is doubtful that the proxy record from any single sediment archive can reliably determine the rate at which the modern Sahara Desert was established.

Because changes in Saharan humidity are largely driven by the northwards penetration of the monsoon, the duration of humid periods can be expected to vary by latitude, with northern sites experiencing a later onset and earlier termination, than those in the south. Both Kuper and Kröpelin (2006) and Shanahan et al., (2015) provide evidence for this behavior in various lake and marine records from different parts of Africa. However, marine records of dust deposition off the North African coast contradict this picture, showing a rapid rise in dust flux at ~5 ka irrespective of latitude, indicating a swift collapse of the monsoon across the Sahara (McGee et al., 2013). Palaeolake Shati provides a record of the end of the Holocene humid period that lies considerably further north (27° N) than previously studied palaeolake records, and might therefore be expected to experience an earlier desiccation. However, along with most other palaeolakes in the Fezzan, it desiccates at ~5 ka (Cremaschi and Zerboni 2009). Because palaeolakes are important sources of atmospheric dust (Bullard et al., 2011), these lakes potentially provided dust to the Atlantic, contributing to the high dust flux recorded in marine cores at this time (McGee et al., 2013). Nonetheless there is abundant evidence for aridification well before this final drying of Palaeolake Shati at 5.3 ka, which may

have predisposed the lake to final desiccation during subsequent periods of increased aridity. In the Fezzan, the thousand years of aridification prior to 5 ka had shrunk many of the lakes, meaning that additional aridification at 5 ka caused rapid desiccation of many lakes in the region. This mechanism, if applicable to other Saharan basins, potentially explains the rapid rise in dust flux to the Atlantic at 5 ka.

4.3 Validation of LEI using Palaeoclimate and Sediment Records

The evaluation of the lake records presented above allows a limited assessment of the utility of the LEI. When considering sedimentation rates and comparing Palaeolakes Shati and Germa, Palaeolake Shati has the second highest LEI of all lakes in the region and has the highest sedimentation rate, with a 4 m core spanning ~1.9 ka, providing a sedimentation rate of ~2 m/ka. Palaeolake Germa has a lower LEI than Shati, though it is still much higher than most other lakes in the region, having the 14th highest LEI out of 816 lakes. It experiences a lower sedimentation rate, with 3 m of sedimentation in 3 ka, providing a rate of 1 m/ka. Both lakes have the potential for a substantial sedimentary record. Assuming constant sedimentation rates and lake initiation at 11 ka (based on the spring deposits of Wadi el-Agial), then the Holocene record for Paleolake Shati should be 12 m and Paleolake Germa 8m. In contrast, many of the lakes in the Murzuk Sand Sea and the Erg Uan Kasa have very low LEI values and also preserve much less sediment, with lake sediment outcrops varying from a few tens of centimeters to about two meters (Cremaschi and Di Lernia 1999).

When considering the length of time a lake contains water, the LEI appears to perform less well. Paleolake Germa has a lower LEI than Palaeolake Shati, yet it persists for longer after the onset of aridity. This longevity is explained by substantial groundwater inputs into the lake, a factor not considered by the LEI. These results suggest that the LEI has limited utility in predicting lake longevity. However, Palaeolake Germa is atypical, receiving groundwater discharge along a 100 km long discharge zone from the largest aquifer in the Fezzan Basin. To draw firm conclusions on the utility of the LEI method, it needs to be evaluated on more lakes.

5 Conclusion

The catchment-based approach to palaeoclimate reconstruction in deserts described here provides an effective method for understanding past climate change, while ameliorating the problems associated with the truncated nature of dryland terrestrial sedimentary archives. Central to our approach is calculation of the LEI, which allows identification of palaeolakes that are likely to preserve long term sedimentary records and thus can be targeted for field study. Our results show that the LEI method correctly discriminates between basins both with and without extensive sedimentary sequences. However, it does not predict the longevity of the lakes particularly accurately, probably because it only considers surface hydrological characteristics, while many lakes in the Fezzan receive significant groundwater inputs.

We selected the Wadi ash Shati and Wadi el-Agial catchments for detailed study as they contained palaeolakes with high LEIs. The spring, delta and palaeolake records of these catchments provide a rich composite record of past climate change spanning the period

from MIS5 to the Holocene, with Palaeolake Shati providing the longest record. During MIS 5 we recognize two lake phases, a larger lake in MIS 5c/d and a slightly smaller lake during MIS 5e. Both of these lakes have a larger areal extent than the one that existed during the Holocene, probably due to the higher insolation maxima during MIS 5, which pulled monsoon rainfall further north and produced longer summer wet seasons. However, the concomitant southward movement of Atlantic Westerly rainfall cannot be discounted, given the evidence from the coquina deposits for a westerly wind direction. If this was the case the lake may have received both summer and winter rainfall. Whatever the cause, the increased humidity during MIS 5c/d and e provided enough water to allow Wadi el-Agial to overspill its catchment and feed moisture into Palaeolake Shati. During the Holocene there was insufficient rainfall for this to occur, providing further evidence that the humid periods during MIS 5 were considerably wetter than that during the Holocene.

Wadi el-Agial and Wadi ash Shati form part of a proposed dispersal corridor for humans across the Sahara during MIS 5 (Drake et al., 2008; Drake et al., 2011). The presence of Middle Palaeolithic-style artefacts on the MIS 5e shore of Palaeolake Shati demonstrates the presence of humans and thus supports the viability of this dispersal route. Furthermore, it supports the findings of other recent studies that show that palaeolake shorelines were suitable for past human occupation and dispersal (e.g. Jennings et al., 2016; Roach et al., 2016; Groucutt et al., 2015; Groucutt et al., 2018).

We find little evidence for humidity in the Fezzan between MIS 5c and the Holocene, which is consistent with other terrestrial records from the central and western Sahara, suggesting that this was dominantly a period of aridity. Humid conditions returned at about 11 ka and groundwater was replenished, producing a 100 km long groundwater discharge zone at the base of the Messak Settafet which initiated the formation of extensive palustrine deposits. These deposits are largely contemporaneous with the growth of spring tufas in the Acacus mountains (Cremaschi et al., 2006). However, deposition of both deposits ceased at ~8.2 ka, when extensive evidence for a period of aridity elsewhere in the tropics has been reported (Mayewski et al., 2004). More humid conditions returned after this arid event; for example, at 7.4 ka Palaeolake Shati was a perennial freshwater lake surrounded by sparsely wooded grasslands. However, neither the Acacus spring deposits nor the Messak Settafet marshes were reactivated, suggesting reduced moisture availability relative to the period before 8.2 ka.

By ~6.5 ka Palaeolake Shati became saline, trees ceased to be a prominent part of the landscape, and a subsequent series of salinity oscillations are observed. The saline interval at about 6 ka in Paleolake Shati is indicative of widespread aridity in the Fezzan, being contemporaneous with a low stand in Palaeolake Germa, the final desiccation of lakes in Murzuk Sand Sea (Cremaschi 1998; Cremaschi and Di Lernia 1998), and an arid period in the Tassili N'Ajjer Mountains (Cremaschi et al., 2006). Both the 8.2 ka and ~6 ka aridity events are concurrent with climatic oscillations noted further afield and are attributed to North Atlantic Ocean cooling (Bond et al., 1997) that caused the collapse of the monsoon. Some hydrological systems which had been active before these arid events, did not reactivate after they ended, suggesting that abrupt drying events occurred in the

context of a gradually drying climate. This aridification is probably explained by declining summer insolation, which caused a weakening of the summer monsoon.

Final desiccation of the Fezzan occurred at ~5 ka. Palaeolake Shati dried up by 5.3 ka, soon followed by the desiccation of most remaining lakes in the sand seas (Cremaschi and Di Lernia1999; Cremaschi 2001). The timing of this aridification is consistent with a substantial body of evidence from other parts of the Sahara (e.g. Armitage et al., 2015; McGee et al., 2013; Nicoll 2004; deMenocal et al., 2000). However, there is much disagreement on the rate of the onset of Saharan aridity, with evidence for both a rapid collapse at about 5 ka (deMenocal et al., 2000; Armitage et al., 2015) and a gradual aridification that started much earlier (e.g. Kröpelin et al., 2008; Ritchie and Haynes 1987). Our results from Paleolake Shati support neither of these theories. Instead we find that drying began at ~6.5 ka, after which the environment experiences arid/humid oscillations until final desiccation at about 5.3 ka. Overall though we find that that abrupt aridity events at ~8.2, and ~6 are superimposed upon an overall drying trend, which culminated in widespread aridification and lake-bed deflation at about 5 ka. Because lakes are prodigious dust sources this potentially explains the rapid rise in dust flux to the Atlantic at 5 ka, this being in part a consequence of longer term aridification. After this time, numerous groundwater fed lakes persisted, following a drying trajectory which was determined by groundwater flux rather than regional palaeoclimate.

Acknowledgements
We thank the Society for Libyan Studies for funding the Fezzan Project and then the Desert Migrations Projects that inspired this work, and funded the fieldwork in the Fezzan and some of the laboratory analyses. Particular thanks go to David Mattingly who led these research projects. Grants from the Leverhulme Trust, National Geographic Society, the University of Benghazi Research Centre, Repsol/YPF Murzuk SA, and the Great Manmade River Authority also funded aspects of this research, for which they are thanked. We also thank Ian Matthews for assisting with the Bayesian modelling of the Wadi ash Shati core. SA's contribution to this work was partly supported by the Research Council of Norway, through its Centres of Excellence funding scheme, SFF Centre for Early Sapiens Behaviour (SapienCE), project number 262618.

References

Alley, R.B., Mayewski, P.A., Sowers, T., Stuiver, M., Taylor, K.C., Clark, P.U., 1997. Holocene climatic instability: A prominent, widespread event 8200 yr ago. Geology 25, 483-486.

Armitage, S. J., Bristow, C. S., Drake, N. A., 2015. West African monsoon dynamics inferred from abrupt fluctuations of Lake Mega-Chad. Proceedings of the National Academy of Sciences U S A 112, 8543-8548.

Armitage, S.J., Drake, N.A., Stokes, S., El-Hawat, A., Salem, M.J., White, K. Turner, P. McLaren, S. J., 2007. Multiple phases of North African humidity recorded in lacustrine sediments from the Fazzan Basin, Libyan Sahara. Quat. Geochronol. 2, 181-186.

Bellair P., Pauphilet D., 1959. L'âge des tombes nréislamioues de Teierhi (Fezzan). Trav. de I'Inst. de Rech. Sahar. XVIII : 183-185.

Benson, L.V., Paillet, F.L., 1989. The use of total lake-surface area as an indicator of climatic change: examples from the Lahontan basin. Quat. Res. 32, 262–275.

Bond, G., Showers, W., Cheseby, M., Lotti, R., Almasi, P., Priore, P., Cullen, H., Hajdas, I., Bonani, G., 1997. A pervasive millennial-scale cycle in North Atlantic Holocene and glacial climates. Science 278,1257-1266.

Breeze, P.S., Drake, N.A., Groucutt, H.S., Parton, A., Jennings, R.P., White, T.S., Clark-balzan, L., Shipton, C., Scerri, E.M.L., Stimpson, C.M., Al-Omari, A., Petraglia, M.D., 2015. Remote sensing and GIS techniques for reconstructing Arabian palaeohydrology and identifying archaeological sites. Quat. Int. 382, 98–119.

Bronk Ramsey, C., 2009. Bayesian analysis of radiocarbon dates. Radiocarbon 51, 337-360.

Brooks, N., Drake, N., MacLaren, S.,White, K., 2003. Studies in Geography, Geomorphology, Environment and Climate, in: Mattingly, D. J. M., Dore, J. and Wilson, A. I. (Eds.), The Archaeology of Fezzan: Synthesis, Society for Libyan Studies, London. vol. 1, pp 37-74.

Bullard, J. E., Harrison, S. P., Baddock, M. C., Drake, N.A., Gill, T. E., McTainsh, G., Sun Y.,2011. Preferential dust sources: A geomorphological classification designed for use in global dust-cycle models, J. Geophys. Res., 116, F04034.

Castañeda, I.S., Schouten, S., Pätzold, J., Lucassen, F., Kasemann, S., Kuhlmann, H. and Schefuß, E., 2016. Hydroclimate variability in the Nile River Basin during the past 28,000 years. Earth Planet. Sci. Lett. 438, 47-56.

Castañeda, I. S., Mulitza, S., Schefuß, E., dos Santos, R. A. L., Damsté, J. S. S., Schouten, S., 2009. Wet phases in the Sahara/Sahel region and human migration patterns in North Africa. Proc. Natl. Acad. Sci. U S A 106(48), 20159-20163.

Charlton, M.B., White, K., 2007 Sensitivity of radar backscatter to desert surface roughness. Int. J. Remote Sens. 27, 1641-1659, DOI: 10.1080/01431160500491740

Cody, R.D., Cody, A.B., 1988. Gypsum nucleation and crystal morphology in analog saline terrestrial environment. Journal of Sedimentary Petrology 58, 247–255.

Cremaschi, M., 2001. Holocene climatic changes in an archaeological landscape. The case-study of the Wadi Tanezzuft and its drainage basin (SW Fezzan, Libyan Sahara). Libyan Studies 32, 5–28.

Cremaschi, M., 1998. Late Quaternary geological evidence for environmental changes in south-western Fezzan (Libyan Sahara), in: Cremaschi, M. and Di Lernia, S. (Eds.), Wadi Teshuinat: Palaeoenvironment and prehistory in south-western Fezzan (Libyan Sahara). Centro Interuniversitario di Ricerca per le Civiltà e l'Ambiente del Sahara Antico, pp.13-47.

Cremaschi, M., Di Lernia, S., 1998. The geoarchaeological survey in central Tadrart Acacus and surroundings (Libyan Sahara): Environment and culture, in: Cremaschi, M. and Di Lernia, S. (Eds.), Wadi Teshuinat: Palaeoenvironment and prehistory in south-western Fezzan (Libyan Sahara). Centro Interuniversitario di Ricerca per le Civiltà e l'Ambiente del Sahara Antico, 243-296.

Cremaschi, M., Di Lernia, S., 1999. Holocene climate change and cultural dynamics in the Libyan Sahara. Afr. Archaeol. Rev. 16, 211-238.

Cremaschi, M. Pelfini, M. Santilli, M., 2006. Cupressus dupreziana: a dendroclimatic record for the middle-late Holocene in the central Sahara. Holocene 16, 293-303.

Cremaschi, M., Zerboni, A., 2009. Early to Middle Holocene landscape exploitation in a drying environment: two case studies compared from the central Sahara (SW Fezzan, Libya). C. R. Geosci. 341, 689-702.

Cremaschi, M., Zerboni, A., Spötl, C., Felletti, F., 2010. The calcareous tufa in the Tadrart Acacus Mt. (SW Fezzan, Libya): an early Holocene palaeoclimate archive in the central Sahara. Palaeogeogr. Palaeoclimatol. Palaeoecol. 287, 81-94.

Cremaschi, M., Zerboni, A., 2011. Human communities in a drying landscape. Holocene climate change and cultural response in the Central Sahara, in: Martini, I. P., Chestworth, W. (Eds.), Landscape and societies, selected cases, Springer: New York, 67–89,

deMenocal, P.B, Ortiz, J., Guilderson, T., Adkins, J., Sarnthein, M., Baker, L., Yarusinski, M., 2000. Abrupt onset and termination of the African Humid Period: Rapid climate response to gradual insolation forcing. Quat. Sci. Rev, 19, 347-361.

Drake, N.A**.** Breeze, P., Parker, A. 2013. Palaeoclimate in the Saharan and Arabian Deserts during the Middle Palaeolithic and the potential for hominin dispersals, Quat. Int. 300, 48-61.

Drake, N.A., Blench, R.M., Armitage, S.J., Bristow, C.S., White K.H., 2011. Ancient watercourses and biogeography of the Sahara explain the peopling of the desert, Proc. Natl .Acad. Sci. U S A 108, 458-462

Drake, N.A., El-Hawat, A.S., Turner, P., Armitage S.J., Salem, M.J., White, K.H., McLaren S., 2008. Palaeohydrology of the Fazzan Basin and Surrounding Regions: the Last 7 Million Years, Palaeogeogr. Palaeoclimatol. Palaeoecol. 263, 131–145.

Drake, N.A., Wilson, A., Pelling, R., White, K.H., Mattingly, D., Black. S., 2004. Water Table Decline, Springline Desiccation and the Early Development of Irrigated Agriculture in the Wādī al-Ajāl , Libyan Fazzan. Libyan Studies 35, 95-112.

Drake, N.A., White, K., McLaren, S., 2006. Quaternary Climate Change in the Germa Region of the Fezzan, Libyan, in Mattingly, D. (Ed.) Environment, Climate and Resources of the Libyan Sahara, Society for Libyan Studies, London 133-144.

Ehrmann, W., Schmiedl, G., Beuscher, S., Krüger, S., 2017. Intensity of African Humid Periods Estimated from Saharan Dust Fluxes. PloS one 12(1), p.e0170989.

Enzel, Y., 1992. Flood frequency of the Mojave River and the formation of late Holocene playa lakes, southern California. Holocene 2, 11–18.

Fleitmann, D., Burns, S.J., Mudelsee, M., Neff, U., Kramers, J., Mangini, A., Matter, A., 2003. Holocene forcing of the Indian monsoon recorded in a stalagmite from Southern Oman. Science 300, 1737-1739.

Gasse, F., 1977. Evolution of Lake Abhé. Nature 256, 42–45.

Gasse, F., 2000. Hydrological changes in the African tropics since the last glacial maximum. Quat. Sci. Rev. 19, 189–211.

Gaven, C., Hillaire-Marcel, C., Petit-Maire, N. 1981. A Pleistocene lacustrine episode in southeastern Libya. Nature 290, 131-133.

Geyh, M. A., Thiedig, F., 2008. The Middle Pleistocene Al Mahrúqah Formation in the Murzuq Basin, northern Sahara, Libya evidence for orbitally-forced humid episodes during the last 500,000 years. Palaeogeogr. Palaeoclimatol. Palaeoecol. 257, 1-21.

Grandi, G. T., Lippi, M. M., Mercuri, A. M., 1998. Pollen in dung layers from rockshelters and caves of Wadi Teshuinat (Libyan Sahara), in: Cremaschi, M. and Di Lernia, S. (Eds.), Wadi Teshuinat: Palaeoenvironment and prehistory in south-western Fezzan (Libyan Sahara). Centro Interuniversitario di Ricerca per le Civiltà e l'Ambiente del Sahara Antico, pp. 95-106.

Groucutt, H.S., Shipton, C., Alsharekh, A., Jennings, R., Scerri, E.M., Petraglia, M.D., 2015. Late Pleistocene lakeshore settlement in northern Arabia: middle Palaeolithic technology from Jebel Katefeh, Jubbah. Quat. Int. 382, 215-236.

Groucutt, H.S., Grün, R., Zalmout, I.S., Drake, N.A., Armitage, S.J., Candy, I., Clark-Wilson, R., Louys, J., Breeze, P.S., Duval, M., Buck, L.T., Kivell, T., Pomeroy, E., Stephens, N., Stock, J.T., Stewart, M., Price, G.J., Kinsley, L., Sung, W.W., Alsharek, A., Al-Omari, A., Zahir, M., Memesh, A.M., Al Murayyi, K.S.M., Zharani, B., Scerri, E.M.L. and Petraglia, M.D., 2018. Homo sapiens in Arabia by 85,000 years ago. Nat. Ecol. Evol. 2, 800-809.

Gupta, A.K., Anderson, D.M., Overpeck, J.T., 2003. Abrupt Changes in the Holocene Asian Southwest Monsoon and Their Links to the North Atlantic. Nature 421, 354-357.

Hamdan, M.A.E., 2000. Quaternary travertines of Wadis Abu Had-Dib Area, eastern desert, Egypt: palaeoenvironment through field, sedimentology, age and isotopic Study. Sedimentology of Egypt 8, 49-62.

Hounslow, M., White, H., Drake, N.A., Salem, M.J., El-Hawat A., McLaren, S.J., Karloukovski, V., Hlal O., 2017. Miocene humid intervals and establishment of drainage networks by 23 Ma in the central Sahara, southern Libya, Gondwana Res. 45, 118-137.

Jennings, R., Parton, A., White, T. S., Clark-Balzan, L., Breeze, P. S., Groucutt, H. S., Parker, A., Drake, N. A., Petraglia, M.D., 2016. Human occupation of the northern Arabian interior during MIS 3. J. Quat. Sci., 31, 953-966.

Kröpelin, S., Verschuren, D., Lézine, A.M., Eggermont, H., Cocquyt, C., Francus, P., Cazet, J.P., Fagot, M., Rumes, B., Russell, J.M., Darius, F., 2008 Climate-driven ecosystem succession in the Sahara: the past 6000 years. Science,320, 765-768.

Kuhlmann, H., Meggers, H., Freudenthal, T., Wefer, G., 2004. The transition of the monsoonal and the N Atlantic climate system off NW Africa during the Holocene. Geophys. Res. Lett., 31.

Kuper, R., Kröpelin, S., 2006. Climate-controlled Holocene occupation in the Sahara: motor of Africa's evolution. Science 313, 803-807.

Lahr, M.M., Armitage, S., Barton, H., Crivellaro, F., Drake, N., Foley, R., Maher, L., Mattingly, D., Salem, M., Stock, J., White, K., 2008. DMP III: Pleistocene and Holocene palaeonvironments and prehistoric occupation of Fazzan, Libyan Sahara. Libyan Studies 39, 263–294.

Lézine, A.M., Hély, C., Grenier, C., Braconnot, P., Krinner, G., 2011. Sahara and Sahel vulnerability to climate changes, lessons from Holocene hydrological data. Quat. Sci. Rev. 30, 3001-3012.

Marshall,M. H., Lamb, H. F., Huws, D., Davies, S. J., Bates, R., Bloemendal, J., Boyle, J., Leng,M. J., Umer, M., Bryant, C. 2011. Late Pleistocene and Holocene drought events at Lake Tana, the source of the Blue Nile. Global Planet. Change 78, 147–161.

Matter, A., Mahjoub, A., Neubert, E., Preusser, F., Schwalb, A., Szidat, S., Wulf, G., 2016. Reactivation of the Pleistocene trans-Arabian Wadi ad Dawasir fluvial system (Saudi Arabia) during the Holocene humid phase. Geomorphology 270, 88-101.

Mayewski, P.A., Rohling, E.J., Stager, J.C., Karlén, W., Maasch, K., Meeker, L.D., Meyerson, E., Gasse, F., Van Kreveld, S., Holmgren, K., Lee-Thorp. J., Rosqvist, G., Rack, F., Staubwasser, M., Schneider, R.R., Steig, E., 2004. Holocene Climate Variability, Quat. Res. 62, 243-255.

Maxwell, T.A., Haynes Jr, C.V., Nicoll, K., Johnston, A.K., Grant, J.A. and Kilani, A., 2017. Quaternary history of the Kiseiba Oasis region, southern Egypt. J. Afr. Earth Sci, 136, 188-200.

McGee, D., Winckler, G., Stuut, J.B.W., Bradtmiller, L.I., 2013. The magnitude, timing and abruptness of changes in North African dust deposition over the last 20,000 yr. Earth Planet. Sci. Lett. 371, 163-176.

Mercuri, A. M., 2008. Human influence, plant landscape evolution and climate inferences from the archaeobotanical records of the Wadi Teshuinat area (Libyan Sahara). J. Arid Environ. 72, 1950-1967.

Migowski C., Stein M., Prasad S., Negendank J. F. W., Agnon A., 2006. Holocene climate variability and cultural evolution in the Near East from the Dead Sea sedimentary record. Quat. Res. 6, 421–431.

Nicoll, K., 2017. A revised chronology for Pleistocene palaeolakes and Middle Stone Age–Middle Palaeolithic cultural activity at Bîr Tirfawi–Bîr Sahara in the Egyptian Sahara. Quat. Int. Corrected proof. In press.

Nicoll, K., 2004. Records of Recent Environmental Change and Prehistoric Human Activity in Egypt and Northern Sudan. Quat. Sci. Rev. 23, 561-580.

Nguetsop F., Bentaleb I., Favier C., Martin C., Servant M., Servant-Vildary S., 2011. Past environmental and climatic changes during the last 7200 cal yrs BP in Adamawa plateau (Northern-Cameroun) based on fossil diatoms and sedimentary 13C isotopic records from Lake Mbalang. Clim. Past 7, 305-345.

Olaka L.A., Odada, E.O., Trauth M.H., Olago D.O., 2010. The sensitivity of East African rift lakes to climate fluctuations. J Palaeolimnol. 44, 629-644.

Petit-Maire, N., Delibrias, G., Gaven, C., 1980. Pleistocene lakes in the Shati area, Fezzan. Palaeoecol. Afr. 12, 289-295.

Petit-Maire, N (Eds.) 1982. Le Shati, lac pléistocène du Fezzan. CNRS, Paris, France, 118 pp.

Pigati, J.S., Rech, J.A., Quade, J., Bright, J., 2014. Desert wetlands in the geologic record. Earth Sci. Rev. 132, 67–81

Roach, N.T., Hatala, K.G., Ostrofsky, K.R., Villmoare, B., Reeves, J.S., Du, A., Braun, D.R., Harris, J.W., Behrensmeyer, A.K., Richmond, B.G., 2016. Pleistocene footprints show intensive use of lake margin habitats by Homo erectus groups. Sci. Rep. 6, 26374.

Ritchie, J. C., Haynes, C. V. 1987., Holocene vegetation zonation in the eastern Sahara. Nature 330, 645-647.

Rohling, E.J., Mayewski, P.A., Hayes, A., Abu-Zied, R.H., Casford, J.S.L., 2002. Holocene atmosphere–ocean interactions: records from Greenland and the Aegean Sea. Climate Dyn. 18, 573– 592.

Shanahan, T.M., Overpeck, J. T., Wheeler, C.W., Beck, J.W., Pigati, J. S., Talbot,M. R., Scholz, C. A., Peck, J., King, J. W., 2006. Palaeoclimatic variations in West Africa from a record of late Pleistocene and Holocene lake level stands of Lake Bosumtwi, Ghana. Palaeogeogr. Palaeoclimatol. Palaeoecol. 242, 287–302.

Shanahan, T.M., McKay, N.P., Hughen, K.A., Overpeck, J.T., Otto-Bliesner, B., Heil, C.W., King, J., Scholz, C.A., Peck, J., 2015. The time-transgressive termination of the African Humid Period. Nat. Geosci. 8, 140–144.

Street F.A., 1980. The relative importance of climate and local hydrogeological factors in influencing lake-level fluctuations. Palaeoecol. Afr. 12,137-158.

Street-Perrott, F.A., Harrison, S.P., 1985. Lake levels and climate reconstruction, in: Hecht, A.D. (Ed.), Palaeoclimate Analysis and Modeling. Wiley, New York, 291–340.

Street-Perrott, F.A., Marchand, D.S., Roberts, N., Harrison, S.P., 1989. Global Lake-Level Variations from 18,000 to 0 Years Ago: A Palaeoclimatic Analysis, In: U.S. Department of Energy Technical Report 46, Washington, D.C. 20545. Distributed by National Technical Information Service, Springfield, VA 22161.

Sultan, M., Sturchio, N., Hassan, F., Hamdan, M., Mahmood, A.M., Alfy, Z.E., Stein, T., 1997. Precipitation source inferred from stable isotopic composition of Pleistocene groundwater and carbonate deposits in the Western desert of Egypt. Quat. Res. 48, 29-37.

Thompson, L.G., Mosley-Thompson, E., Davis, M.E., Henderson, K.A., Brecher, H.H., Zagorodnov, V.S., Mashiotta, T.A., Lin, P.N., Mikhalenko, V.N., Hardy, D.R., Beer, J., 2002. Kilimanjaro ice core records: evidence of Holocene climate change in tropical Africa. Science 29, 589-593.

Tjallingii, R., Claussen, M., Stuut, J.B.W., Fohlmeister, J., Jahn, A., Bickert, T., Lamy, F., Röhl, U., 2008. Coherent high-and low-latitude control of the northwest African hydrological balance. Nat. Geosci. 1, 670-675.

Weldeab, S., Schneider, R.R., Kolling, M., Wefer, G., 2005. Holocene African droughts relate to eastern equatorial Atlantic cooling. Geology 33, 981–984.

White, H.E., 2016. Establishing the Chronostratigraphy and Miocene-Pliocene Palaeoenvironmental History of the Fazzan Basin, Libyan Sahara. PhD Thesis, University of Leicester.

Yechieli, Y., Wood, W., 2002. Hydrogeologic processes in saline systems: playas, sebkhas, and saline lakes. Earth-Sci. Rev. 58, 343–365.

Zielhofer, C., von Suchodoletz, H., Fletcher, W.J., Schneider, B., Dietze, E., Schlegel, M., Schepanski, K., Weninger, B., Mischke, S., Mikdad, A., 2017. Millennial-scale fluctuations in Saharan dust supply across the decline of the African Humid Period. Quat. Sci. Rev. 171, 119-135.

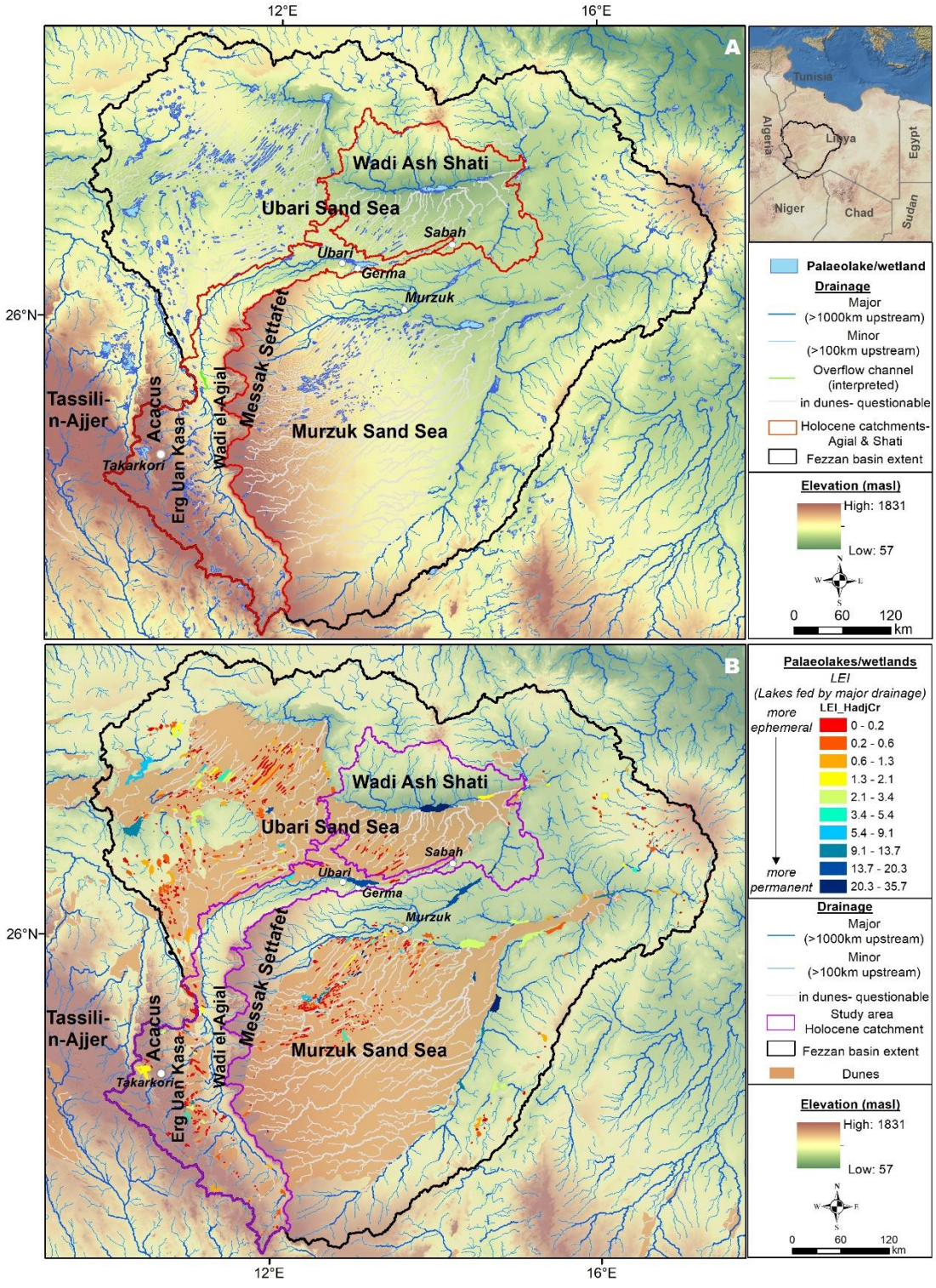

Figure 1. A) DEM of the study area showing the palaeohydrology of the Fezzan and the catchment of Wadi ash Shati and Wadi el-Agial. B) Palaeohydrology of the Fezzan showing the Lake Evaluation Index.

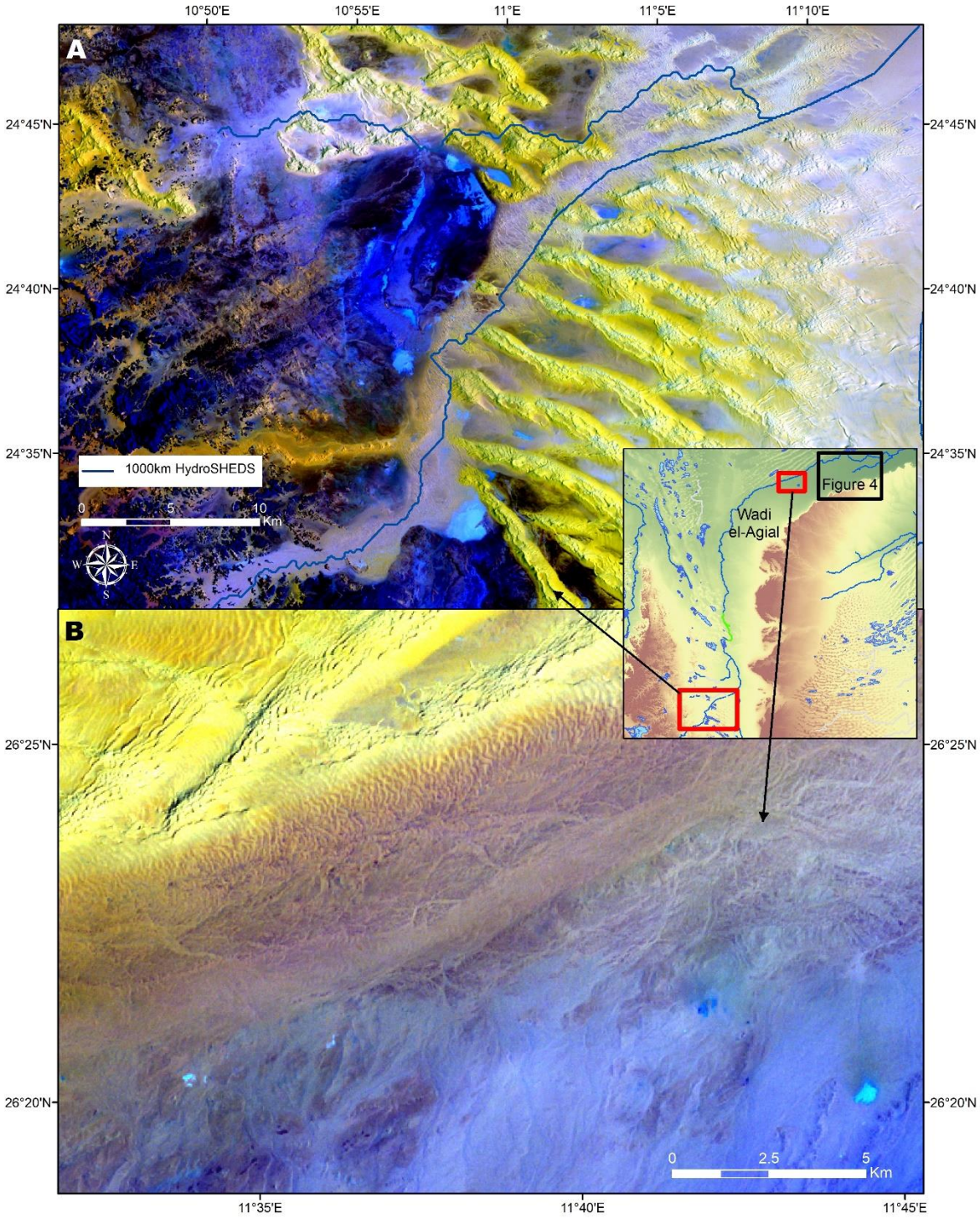

Figure 2. Landsat TM images of different reaches of the Wadi el-Agial. The inset image shows the SRTM DEM and the location of A, B and Fig. 4. A) A tributary identified by

the palaeohydrological mapping draining from the Accacus Mountains and flowing through the sand dunes of the Erg Uan Kasa. Note how the channel cuts through the sand dunes. B) The overfit channel of Wadi el-Agial and numerous smaller channels on the braid plain of the Wadi el-Agial. In the south of the image these channels are augmented by others draining the alluvial fans of the Messak Settafet.

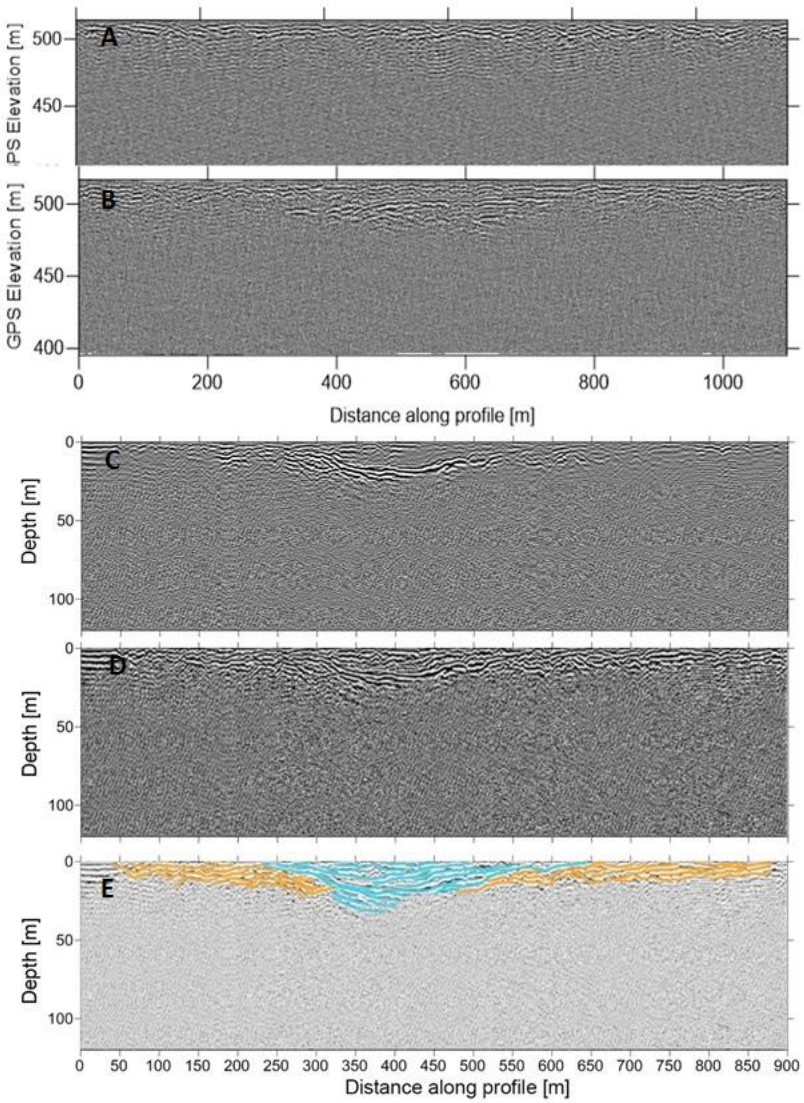

Figure 3. A) Typical profile beneath gravel plain of Wadi el-Agial. B) A 40 m thick near-surface paleochannel. Three processing schemes were employed to produce an enhanced paleochannel image: C) amplitude equalizing filter; D) amplitude equalizing and median filter and E) interpretation of stratigraphy with yellow representing reflections from the primary channel and cyan the cutting and infilling of this unit and the underlying bedrock by a later channel.

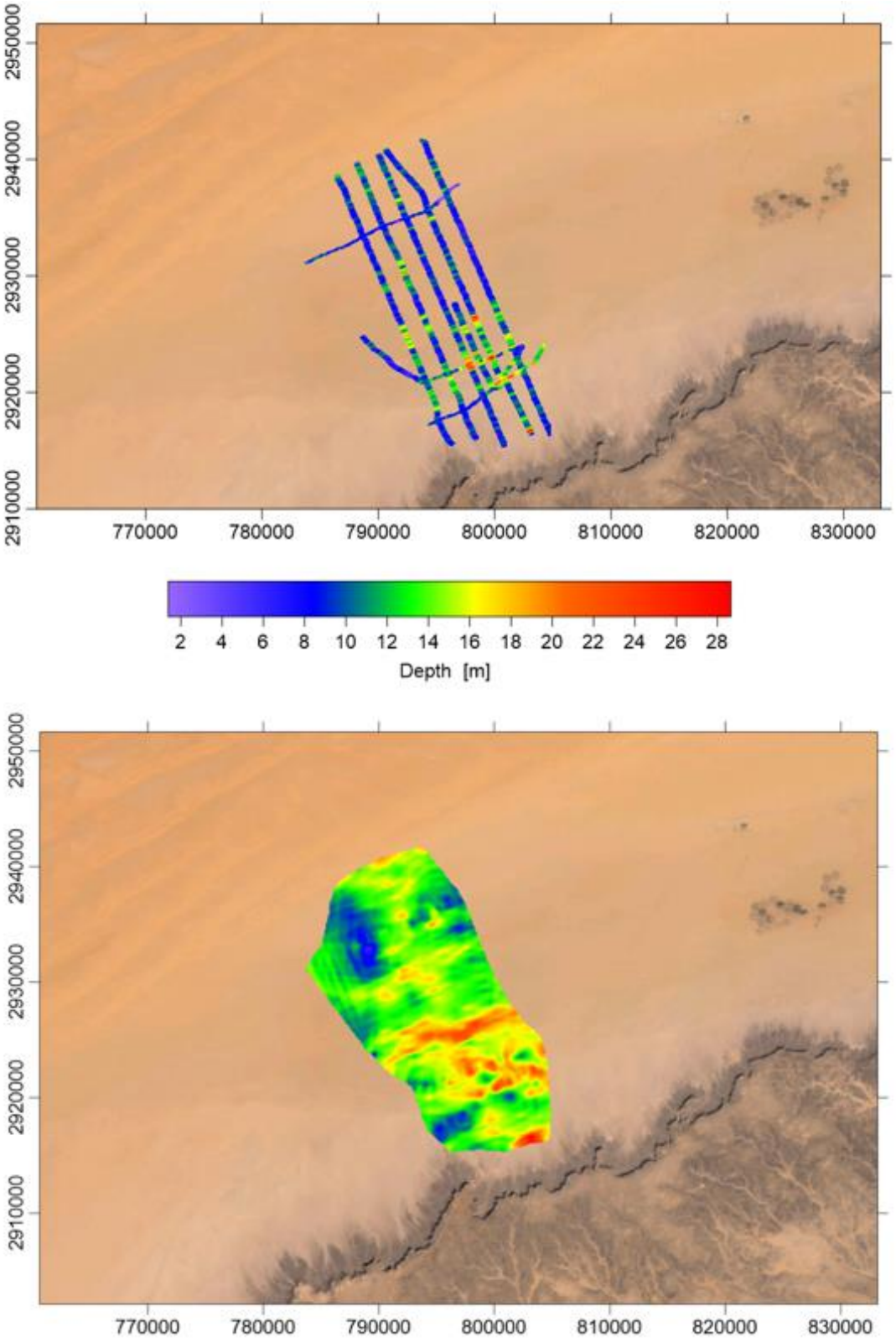

Figure 4. A) Site of the LR GPR parallel profiles on the Wadi el-Agial gravel plain (locaton shown in Figure 2), coloured to show the depth to bedrock and overlain on a Quickbird image. Coordinates are in UTM. B). Interpolated map of depth to bedrock.

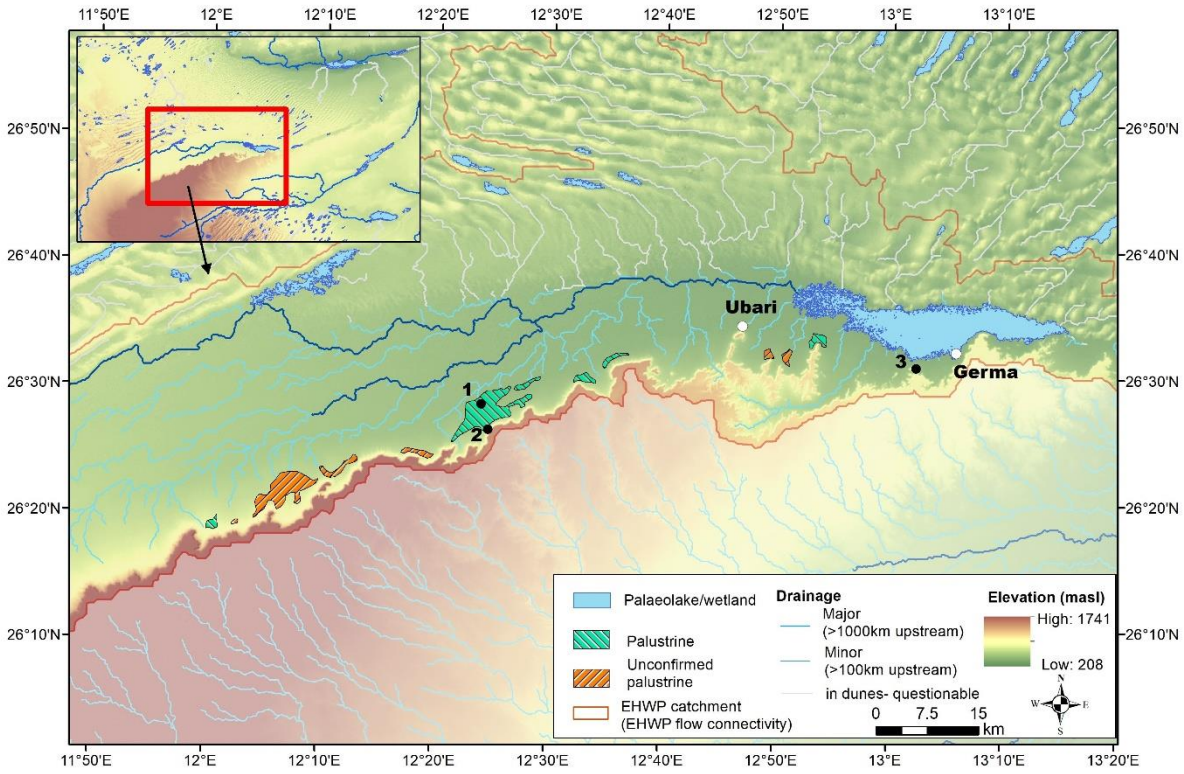

Figure 5. Paleohydrology of Paleolake Germa showing the location of the early Holocene spring deposits and of the stratigraphic sections shown in figure 6. Site 1 is the location of the radiocarbon dated marls, site 2 the location of the dated section west of Ubari shown in Fig. 6 A and 3 the section near Germa.

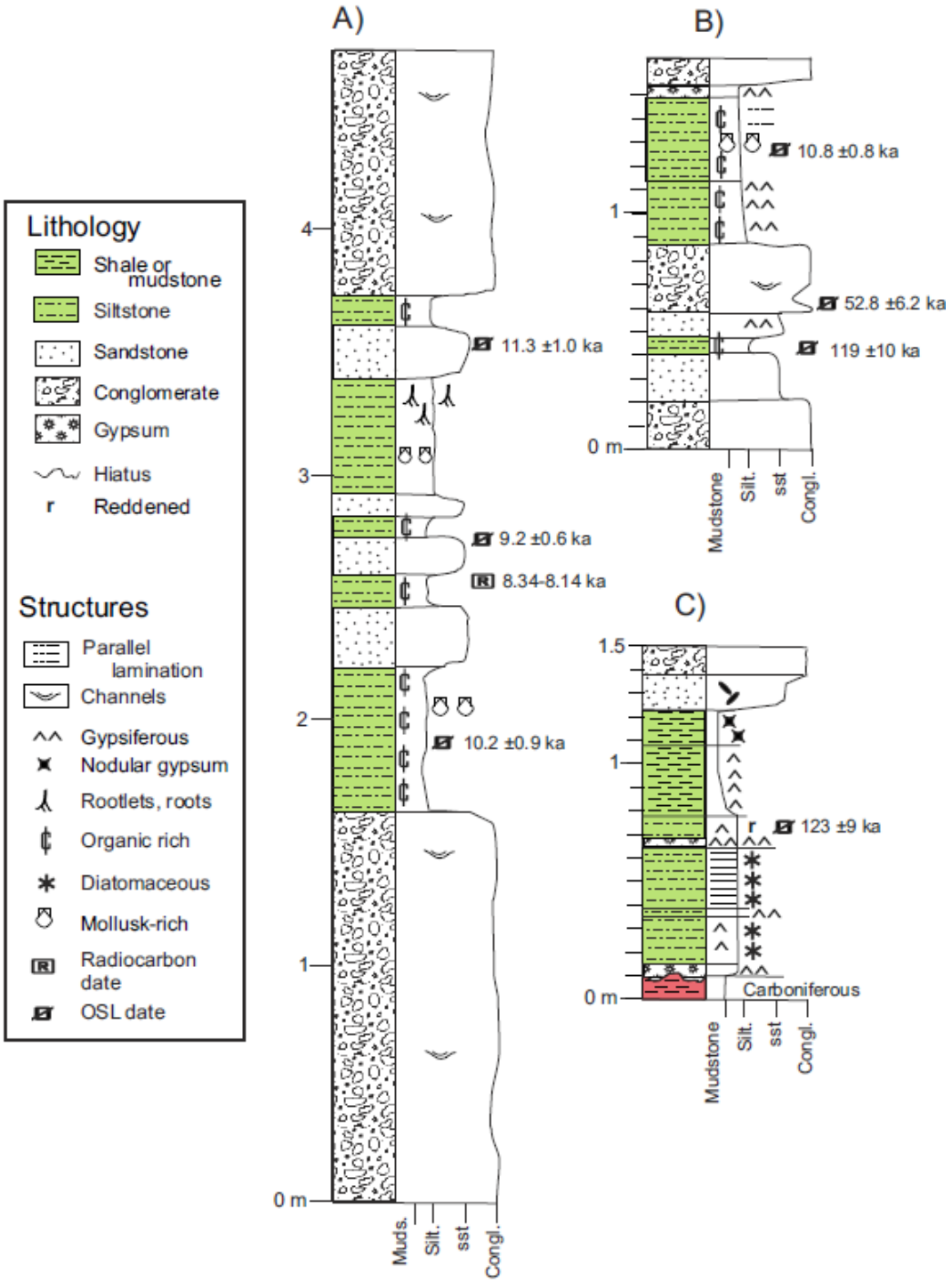

Figure 6. Stratigraphy of palustrine and lacustrine sections. A) Spring fed palustrine deposit west of Ubari. B) Spring fed palustrine deposit near Germa. C) Wadi ash Shati diatomite section.

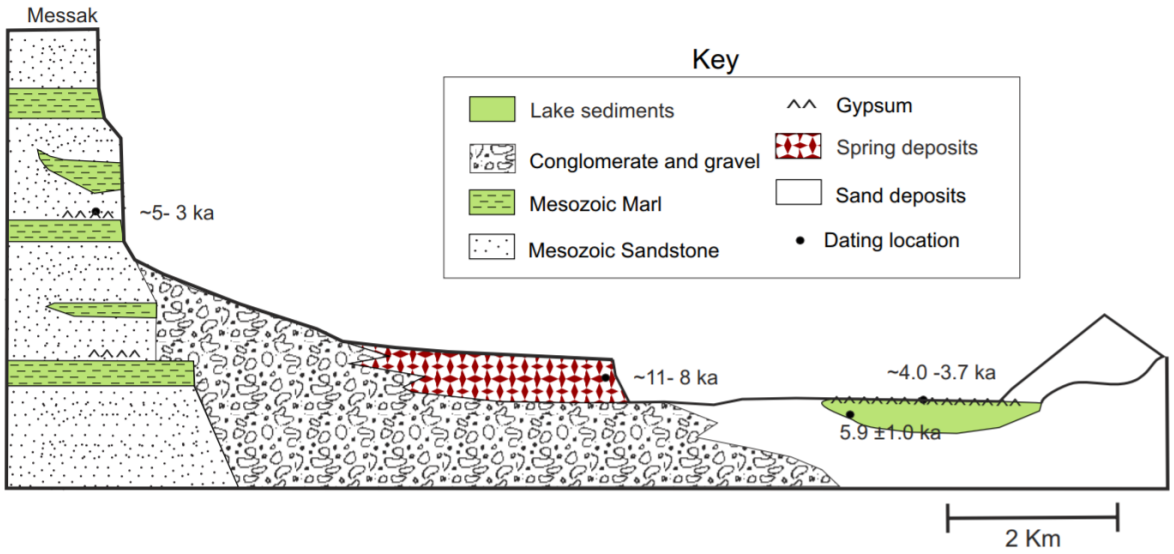

Figure 7. Schematic cross section of Wadi el-Agial valley showing the distribution and age of springs and lakes. Vertical exaggeration is about 0.25.

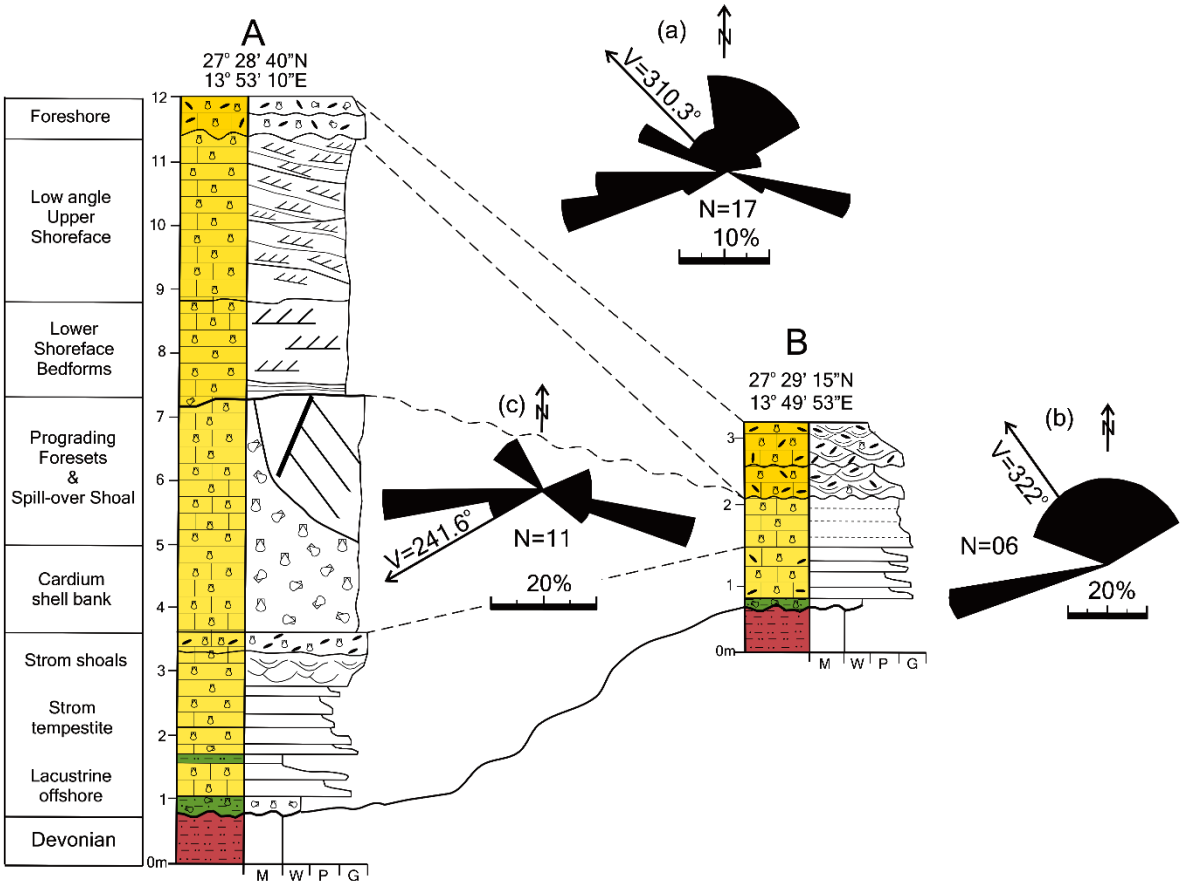

Figure 8. Measured sections at Aqar-1 and Aqar-2 localities showing their correlation and corresponding palaeocurrent rose diagrams. A illustrates the total measured palaeocurrent at both localities whilst B and C show them for specific parts of the sections. The location of these sites is shown in Fig. 9.

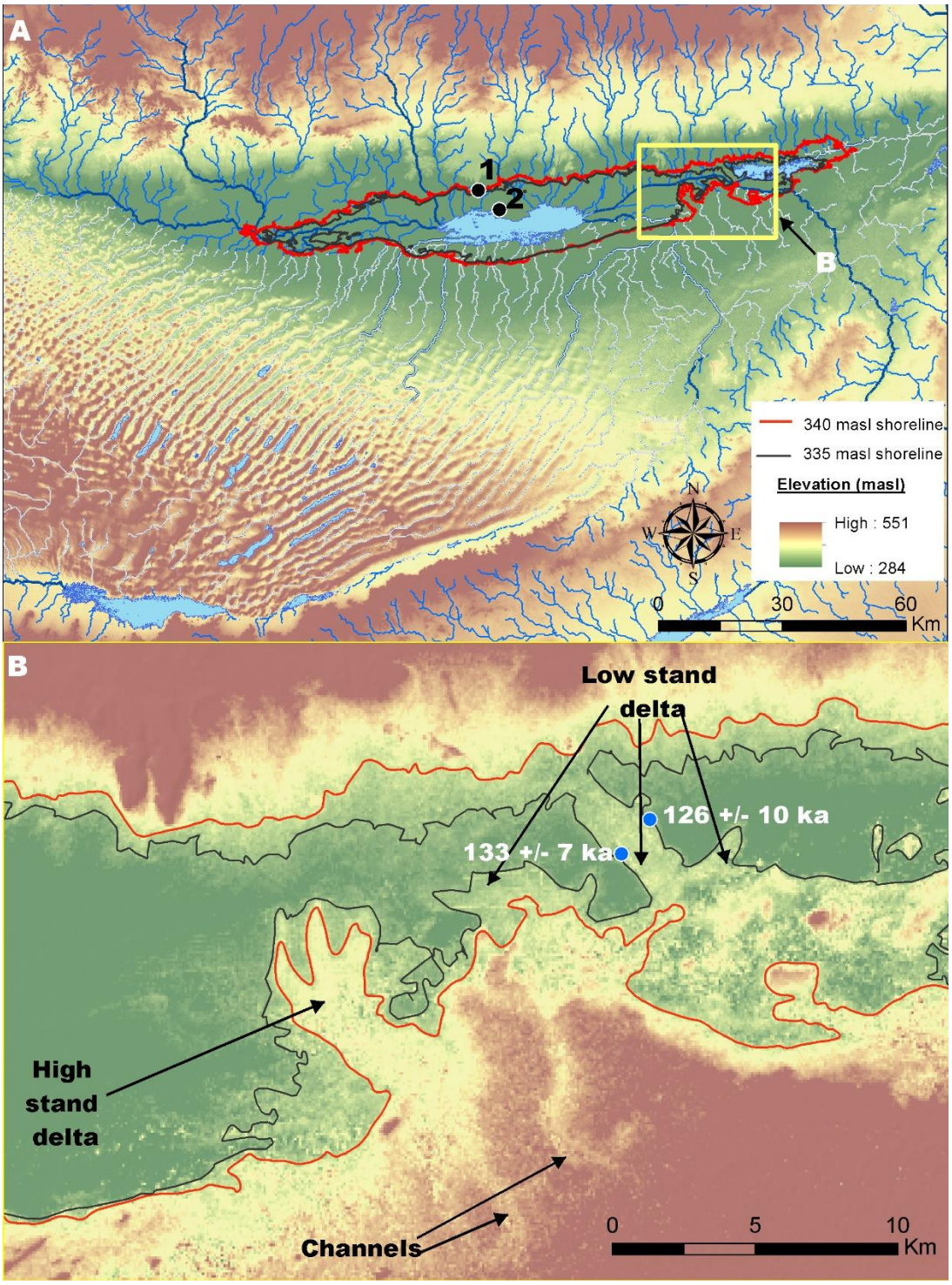

Figure 9. A) Paleohydrology of Wadi ash Shati showing the Holocene lake, the shorelines of the Late Pleistocene lakes, the location of the Aqar 1 and 2 coquina deposits

(1), the diatomite deposit (2), and the location of the Wadi el-Agial deltas shown in more detail in B. B) Topography of the deltas and the OSL dates of the low stand delta.

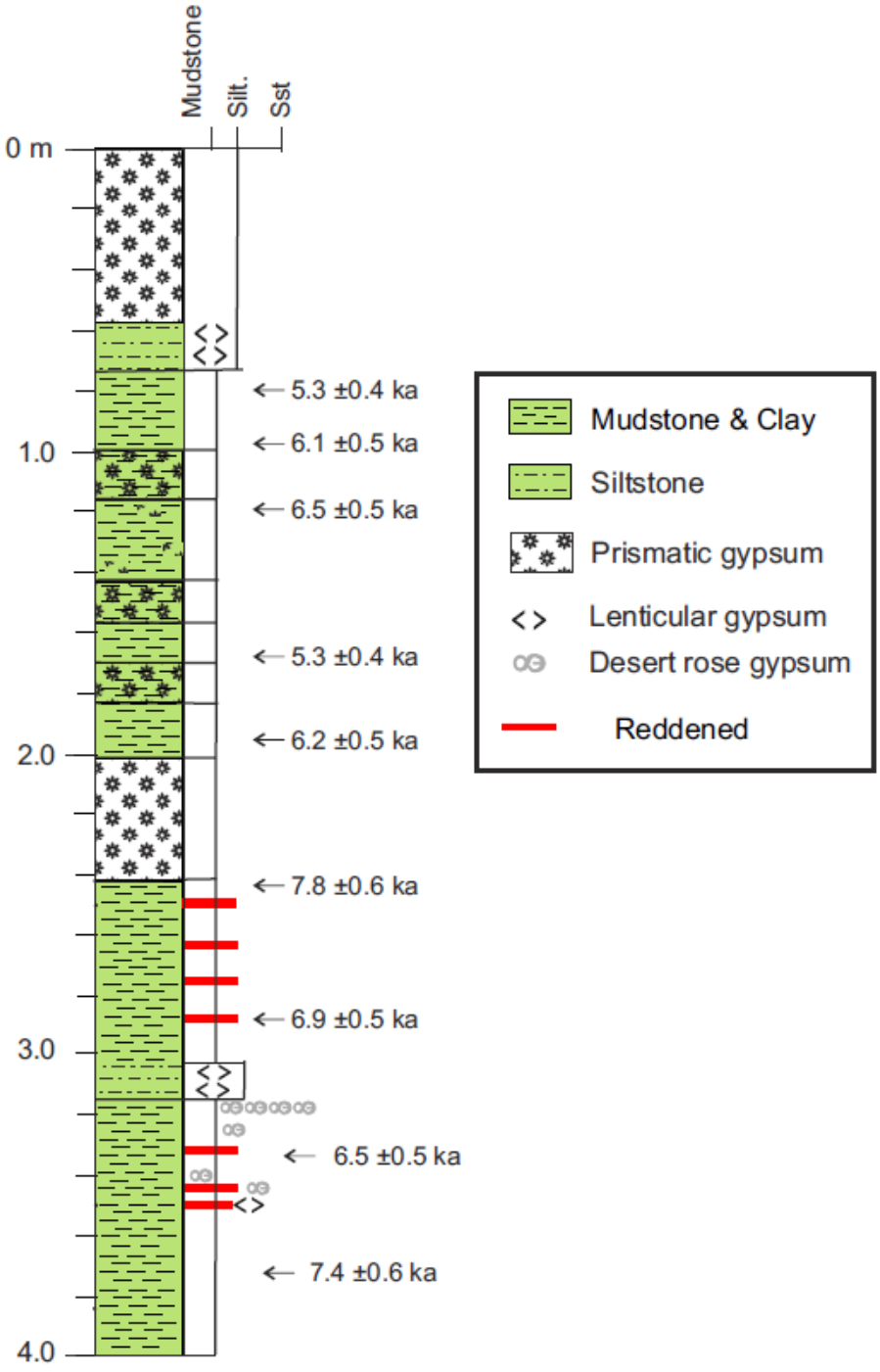

Figure 10. Paleolake Shati core stratigraphy, gypsum crystal form and OSL dates.

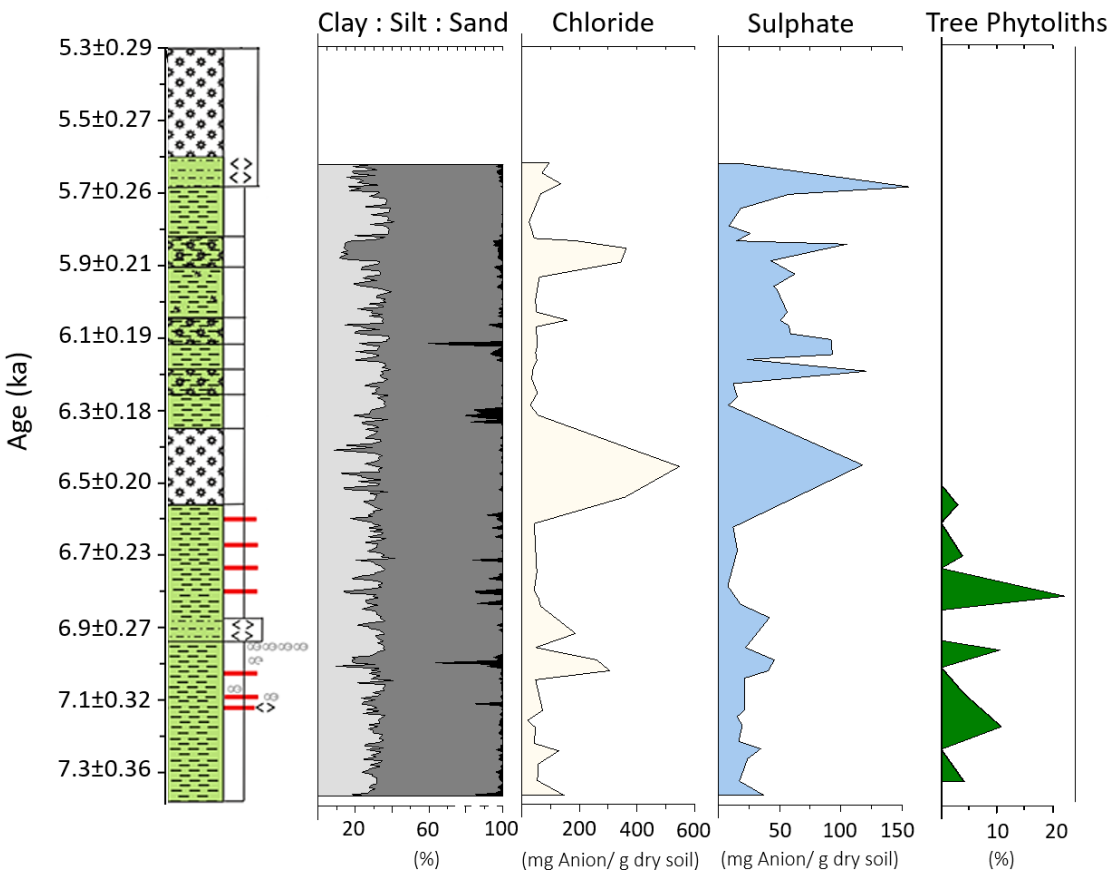

Figure 11. Paleolake Shati stratigraphy with Bayesian age model and down core variations in grain size, chlorine, sulphate and tree phytoliths.